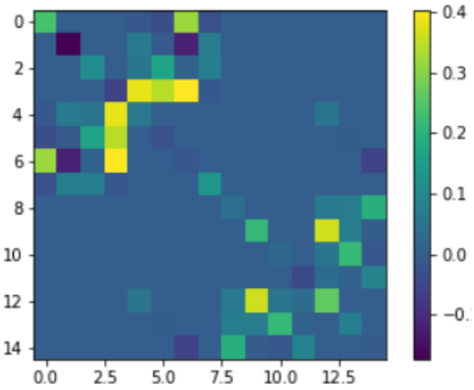

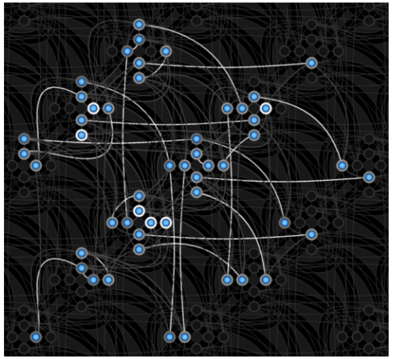

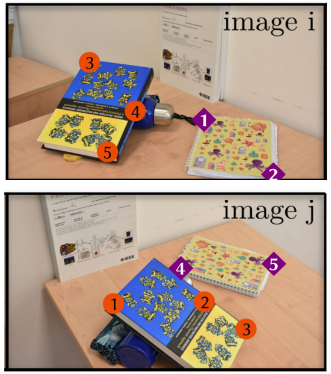

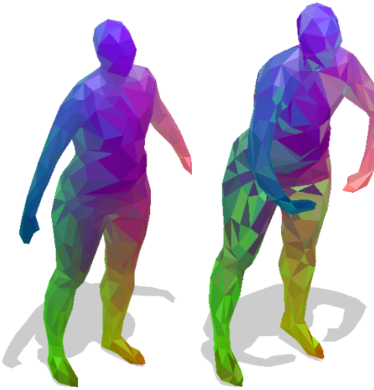

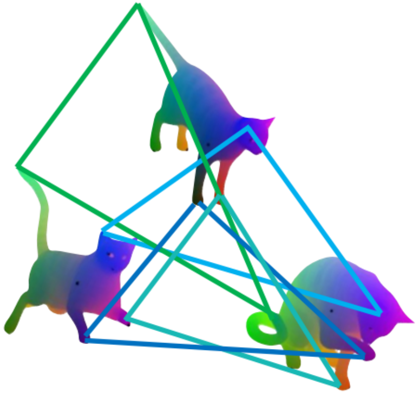

Advances in Quantum Computer Vision

Workshop on Quantum Information (08.12.2022)

UNIVERSITÄT DES SAARLANDES

Vladislav Golyanik

Visual Computing and AI Department

max planck institut informatik

4D and Quantum Vision Group

4D and Quantum Vision (4DQV) Group

- Independent research group integrated in the VCAI Department of MPI for Informatics
- Research agenda at the intersection of CV, CG and ML
- We collaborate in Germany and internationally on these topics

Visual Computing and AI Department

4D and Quantum Vision Group

MPI-INF, Campus E1 4

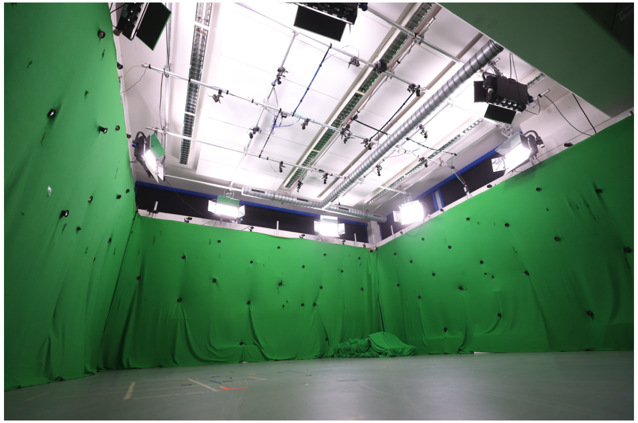

Green-screen Studio

max planck institut informatik

4D and Quantum Vision (4DQV) Group

Two Core Research Areas

Non-rigid 3D (=4D) Perception/Reasoning

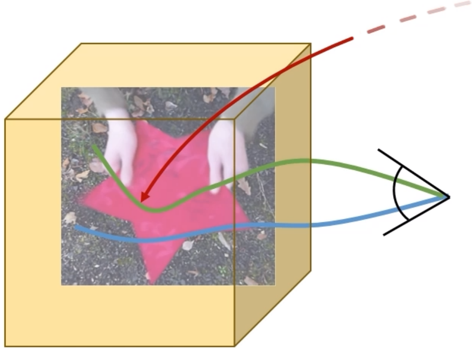

1) explicit and 2) implicit
3D representations

Quantum Computer Vision

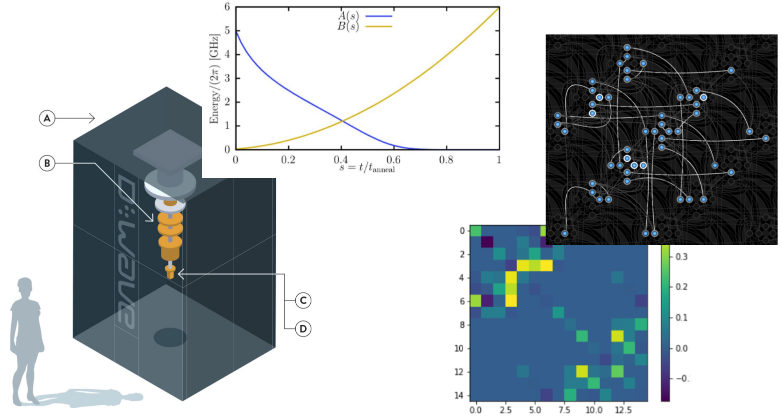

1) What are the relevant problems?
2) Real quantum hardware is in the foreground.

Non-rigid 3D (=4D) Perception/Reasoning

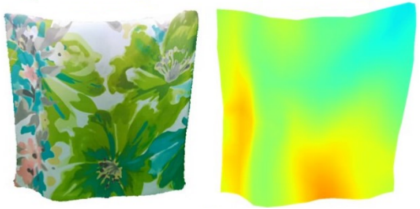

General Objects

Hands

3D Human MoCap (different settings)

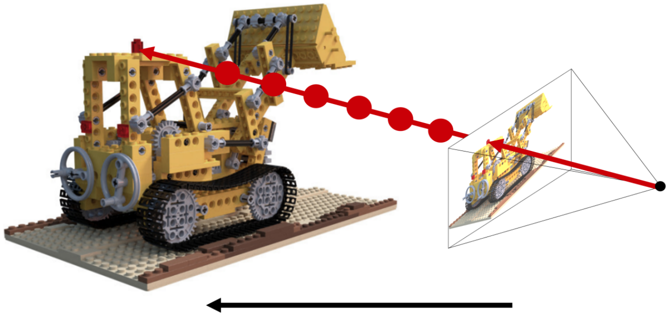

Volumetric 3D Representations

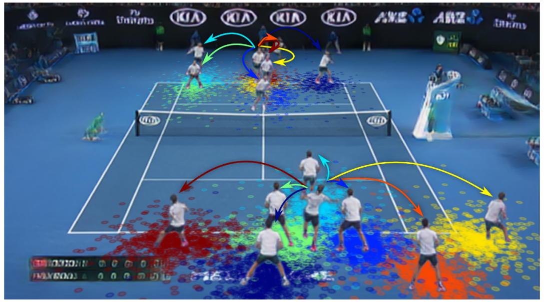

Video/Action Manipulation

Survey: Tretschk and Kairanda et al., arXiv 2022.

Quantum Computer Vision

Problems solved by synchronisation

(Iterative) Matching methods

Quantum Computer Vision

Problems solved by synchronisation

(Iterative) Matching methods

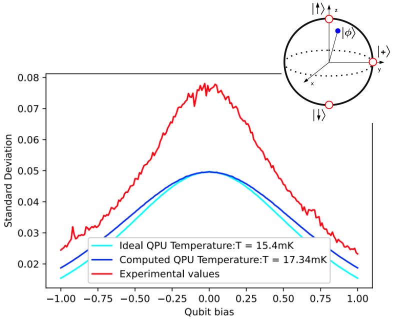

qubit properties

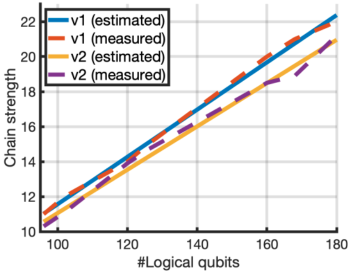

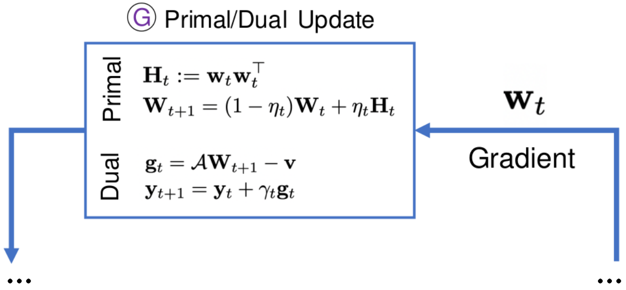

Constrained optimisation

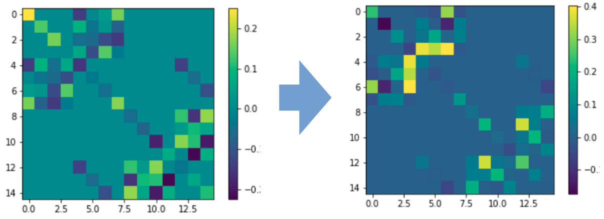

AQC + ML

Methodology of mapping problems to quantum hardware

3D Human MoCap with Physics Priors

Shimada et al., ACM SIGGRAPH 2021.

3D Human-Object Motion Capture

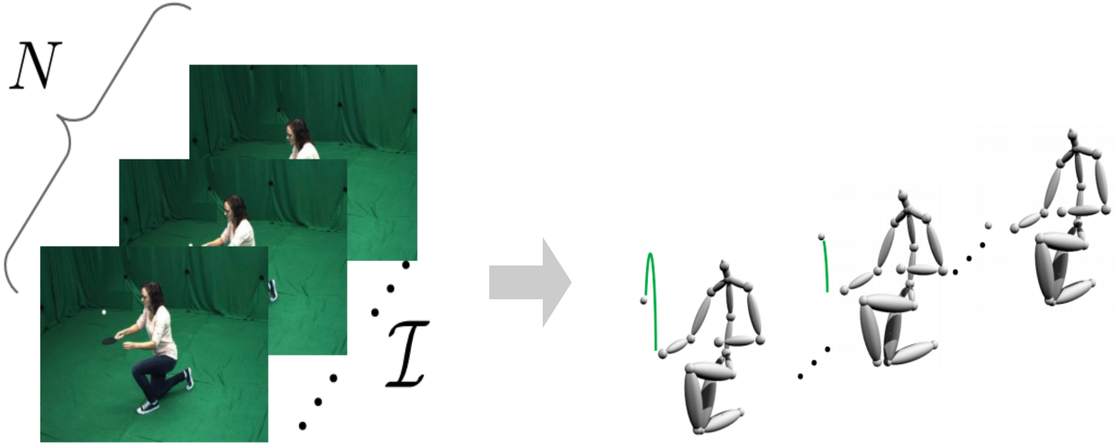

$$x_i = f\frac{X_i}{Z_i} + c_x,\ y_i = f\frac{Y_i}{Z_i} + c_y,\ \forall i,$$

$$\text{s. t.}\quad \sqrt{g_x^2 + g_y^2 + g_z^2} = 9.81\, m/s^2,$$

$$\text{where}\ \begin{cases} X_i = X_0 + u_x t + \frac{1}{2} g_x t^2, \\ Y_i = Y_0 + u_y t + \frac{1}{2} g_y t^2, \quad \text{and} \\ Z_i = Z_0 + u_z t + \frac{1}{2} g_z t^2. \end{cases}$$

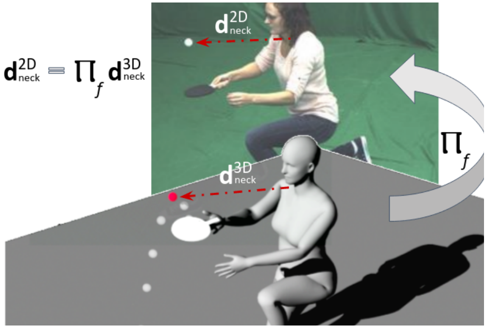

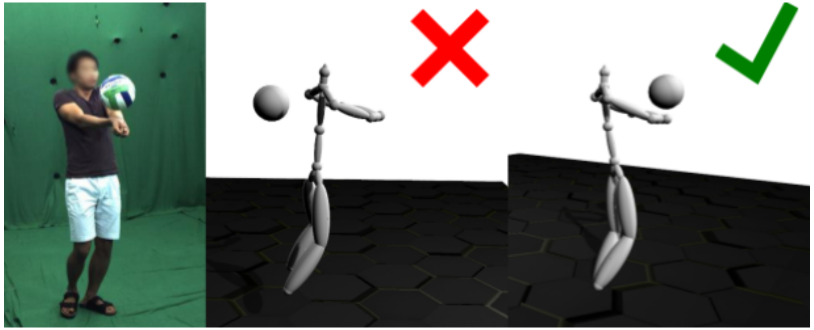

Dabral et al., ICCV 2021.

3D Human MoCap with a Scene Prior

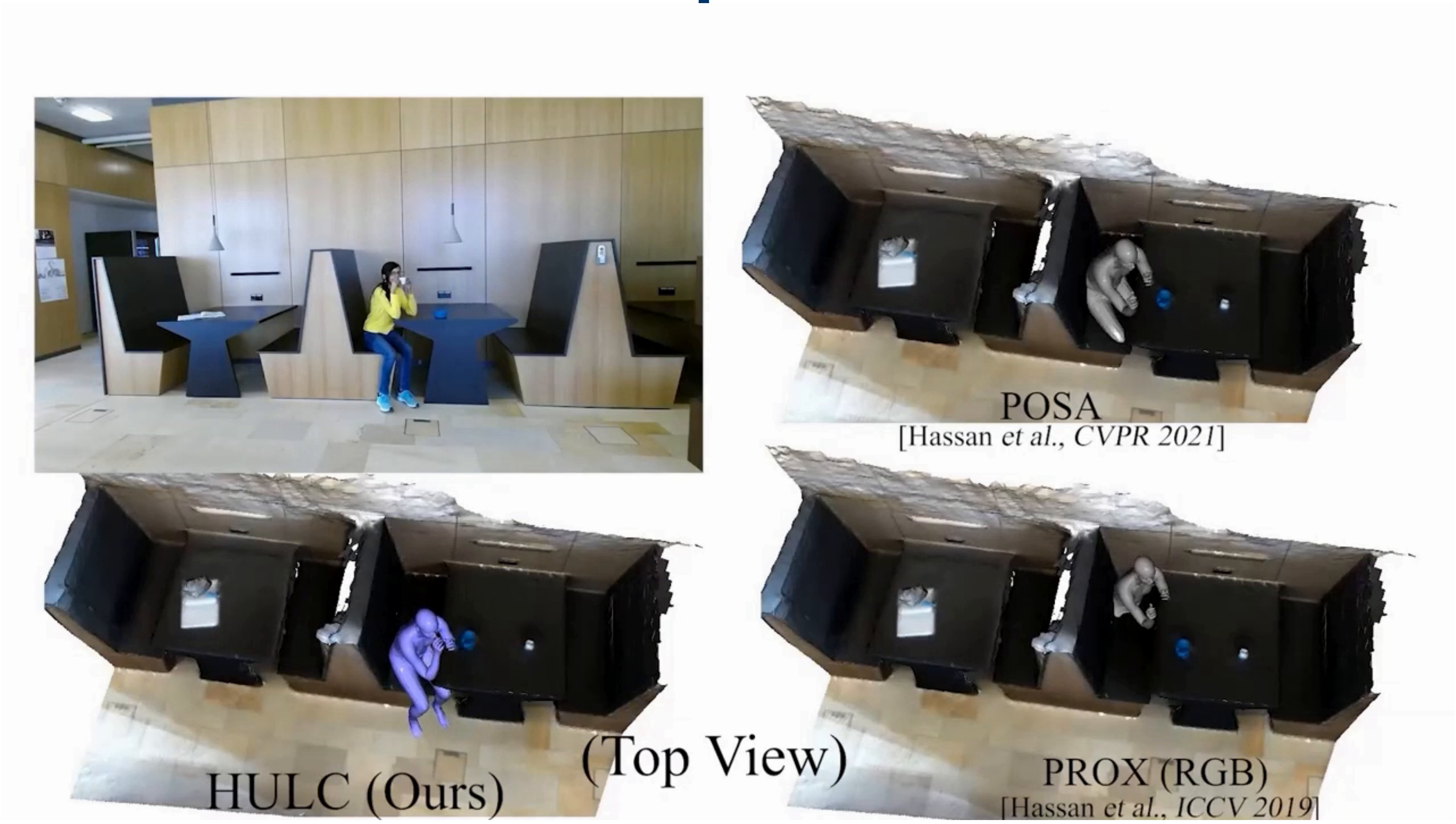

Shimada et al., ECCV 2022.

max planck institut
informatik

3D Human MoCap with a Scene Prior

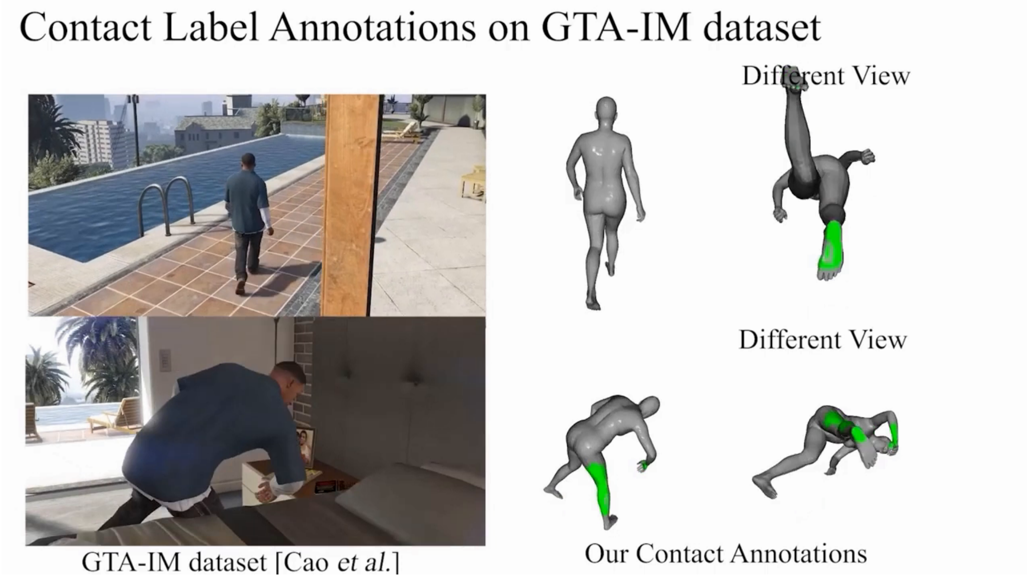

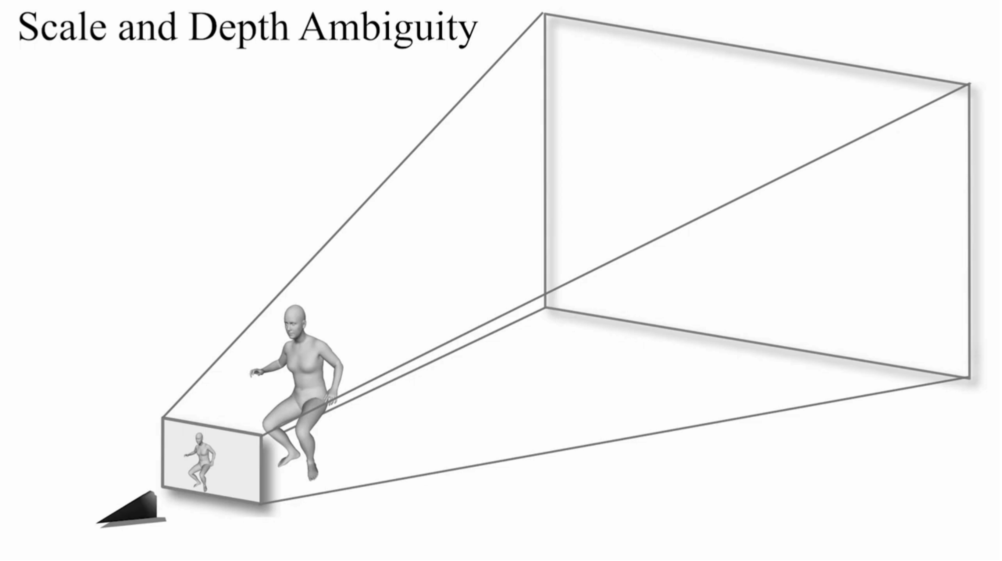

Shimada et al., ECCV 2022.

Playable Environments

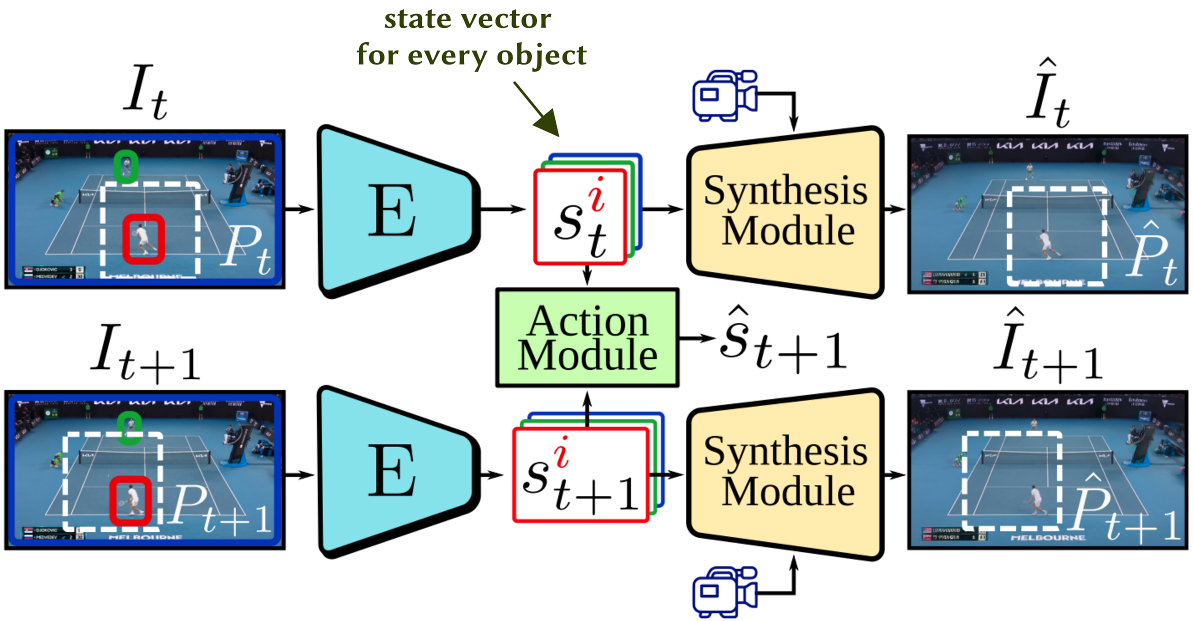

The Approach to Construct Playable Environments (PE)

max planck institut informatik

Menapace et al., CVPR 2022.

Playable Environments

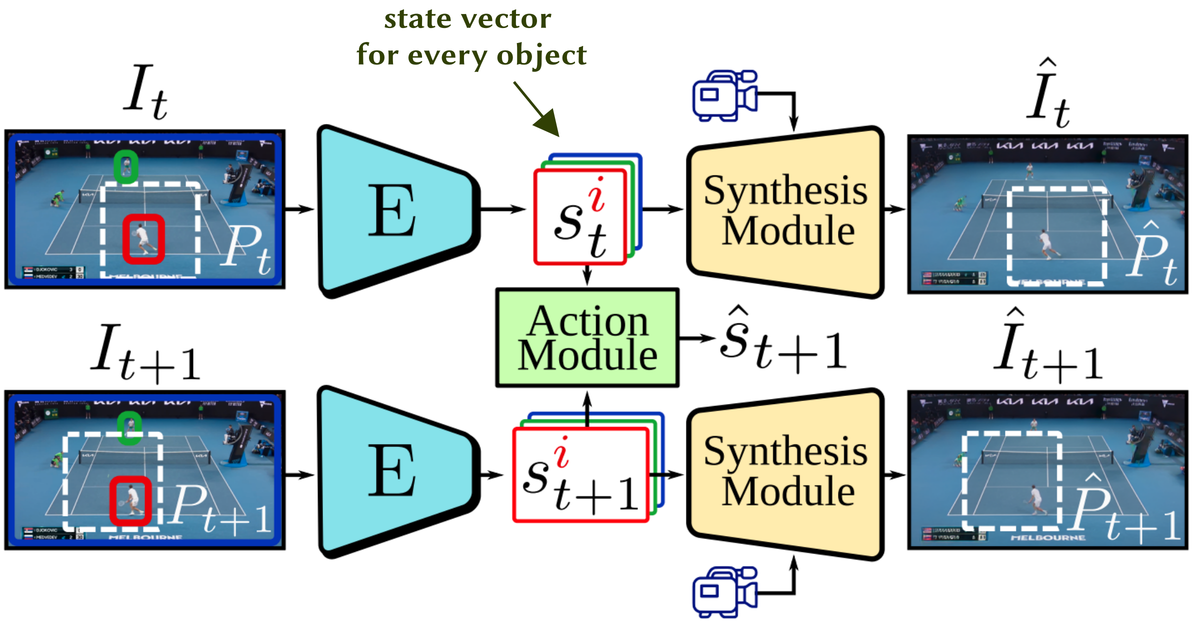

The Approach to Construct Playable Environments (PE)

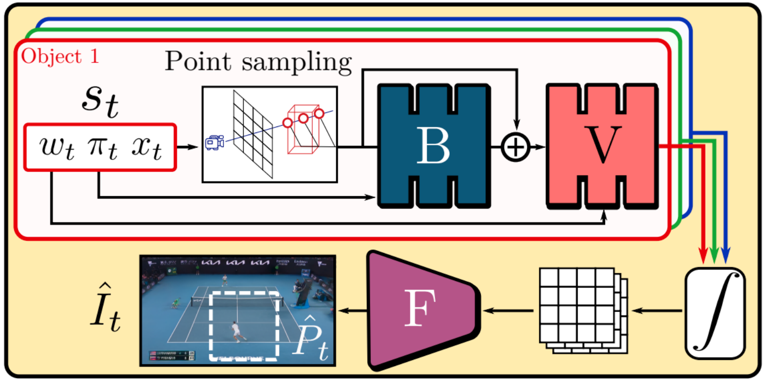

The Synthesis Module

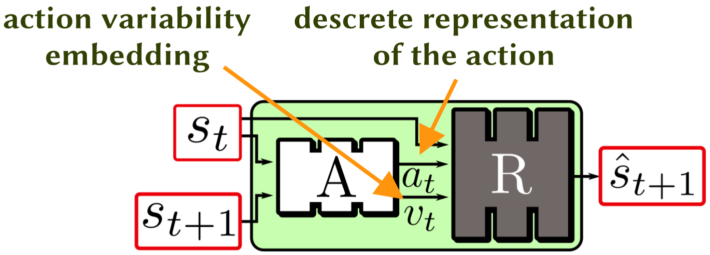

The Action Module

Menapace et al., CVPR 2022.

Playable Environments: Players Control

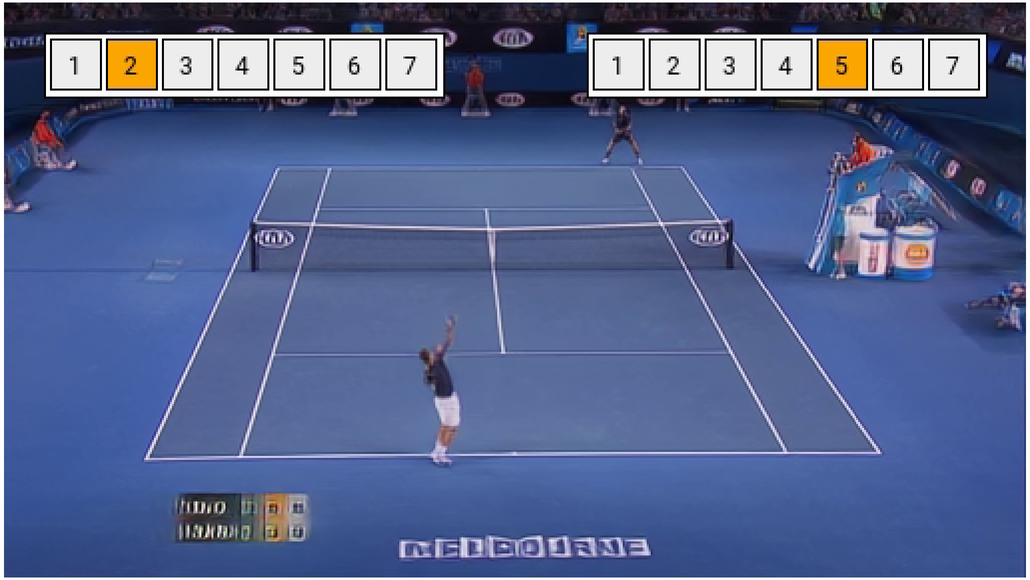

Tennis

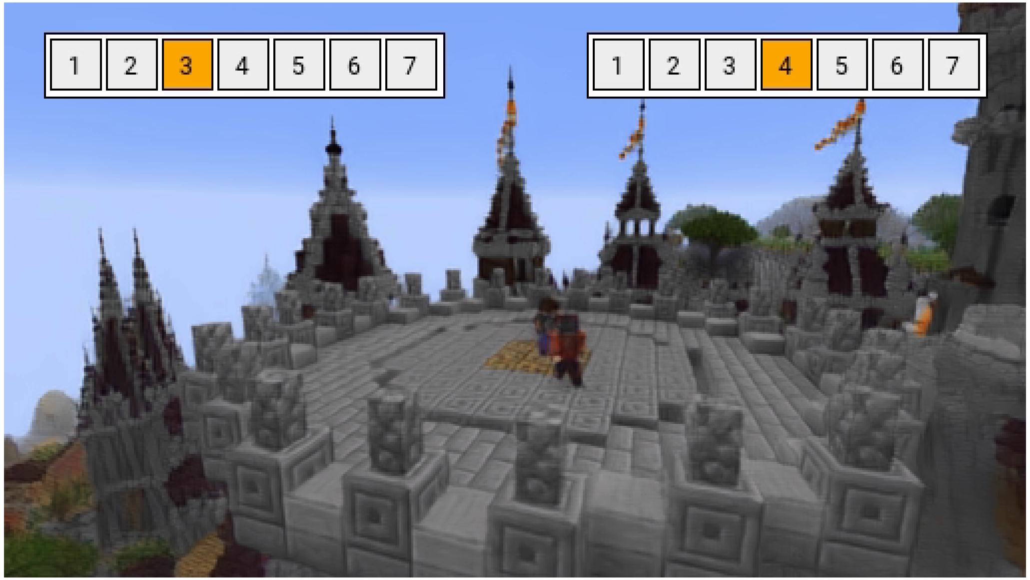

Minecraft

Menapace et al., CVPR 2022.

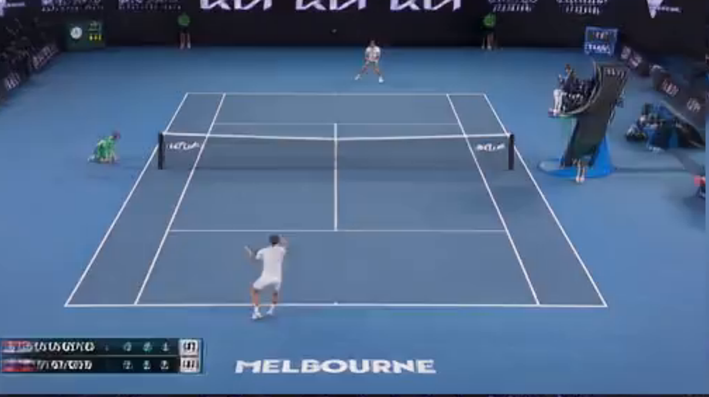
MELBOURNE
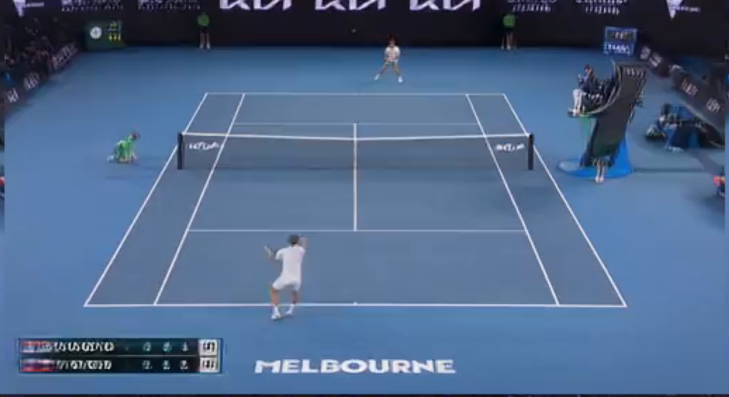
MELBOURNE
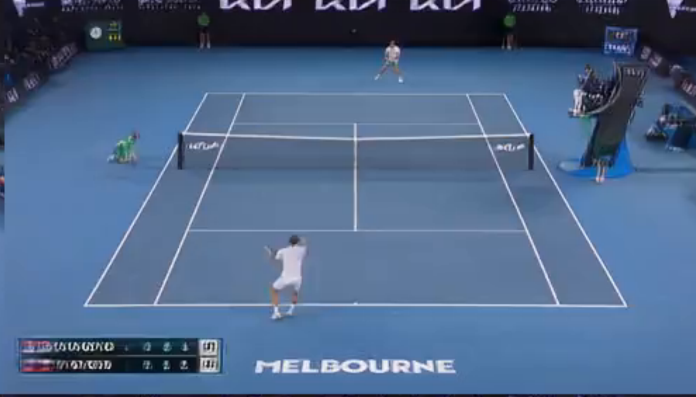
MELBOURNE
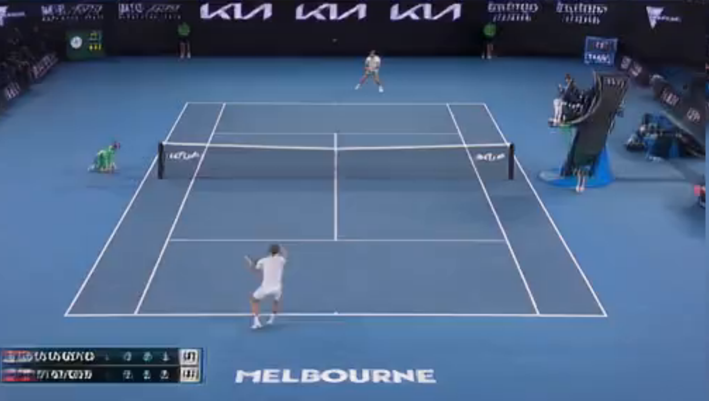
MELBOURNE
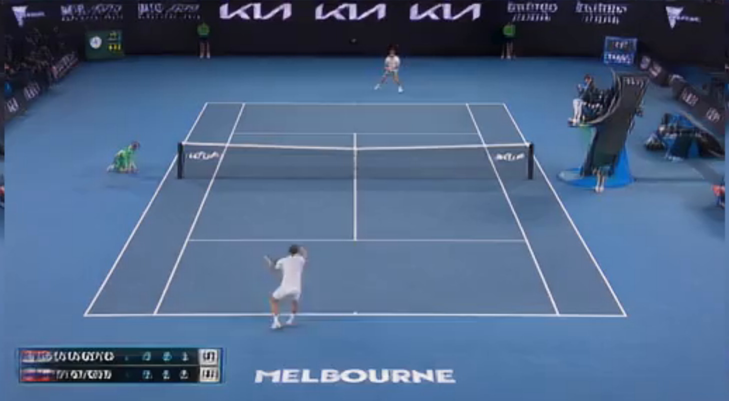
MELBOURNE
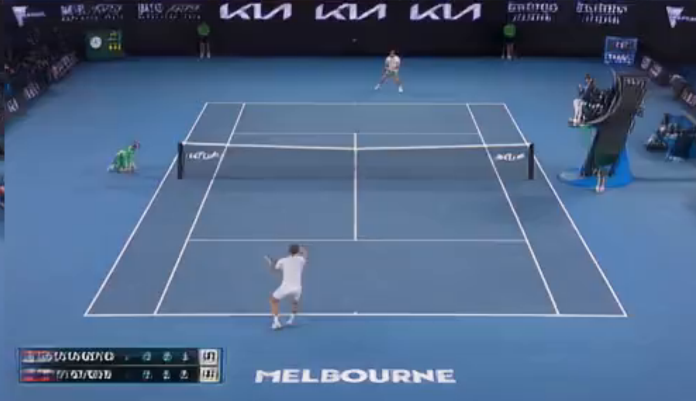
MELBOURNE
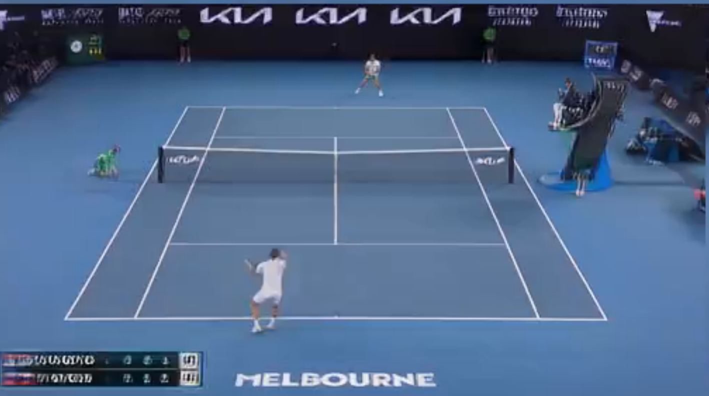
MELBOURNE
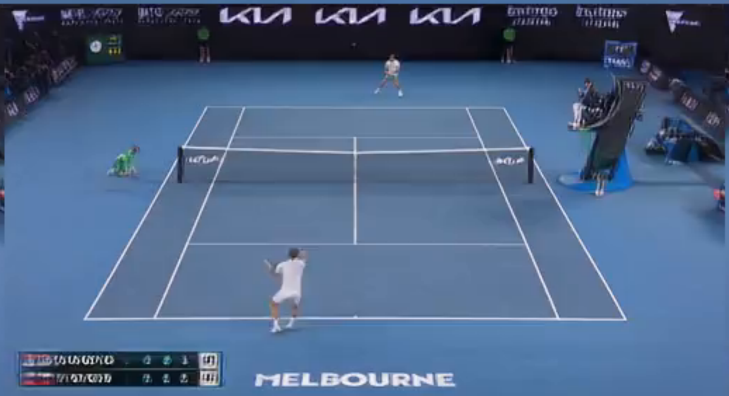
MELBOURNE
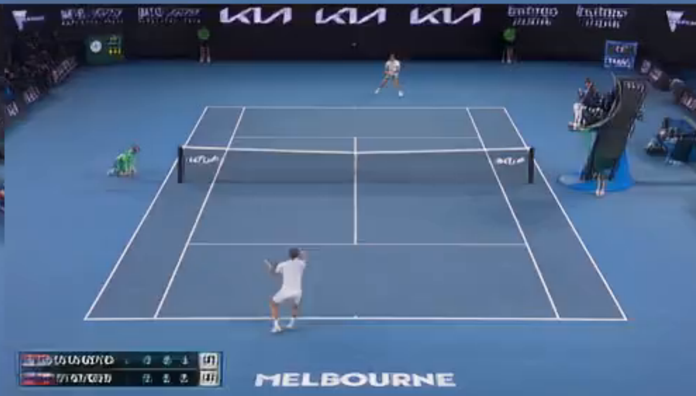
MELBOURNE

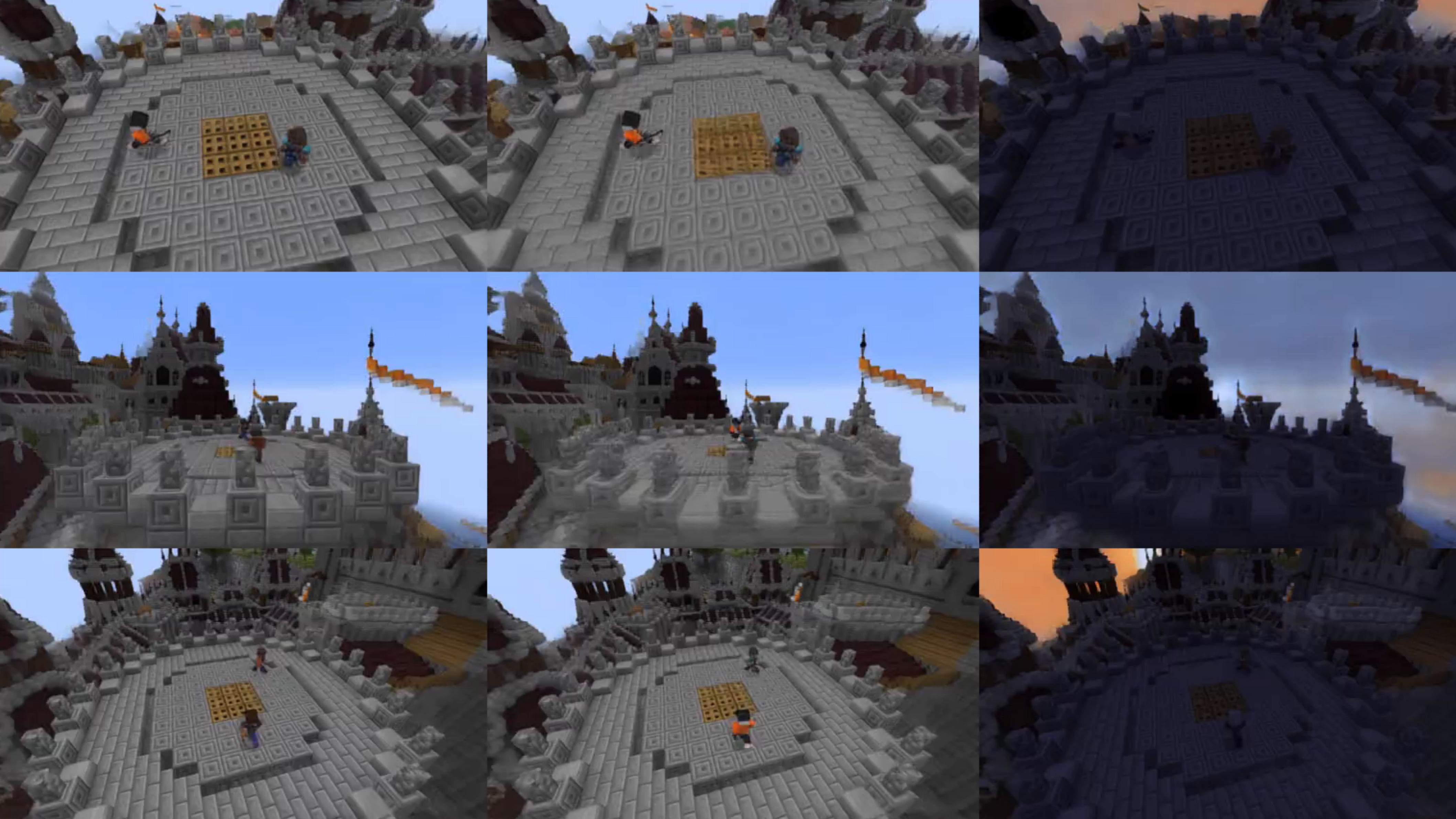

From a Classical to a Quantum Perspective

From a Classical to a Quantum Perspective

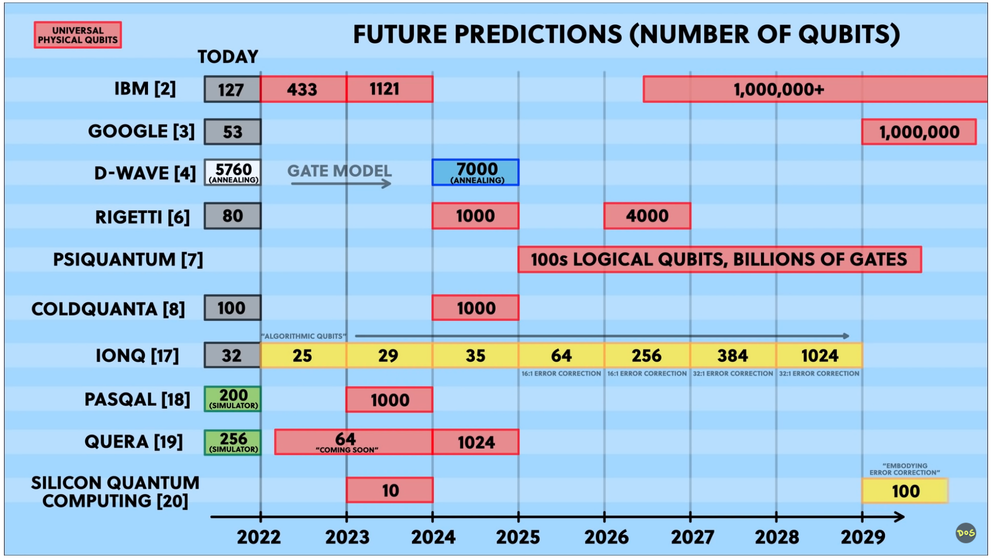

Copyright: D. Walliman. The Map of Quantum Computing, 2022.

- QC are steadily improving
- How can computer vision benefit from QC?

From a Classical to a Quantum Perspective

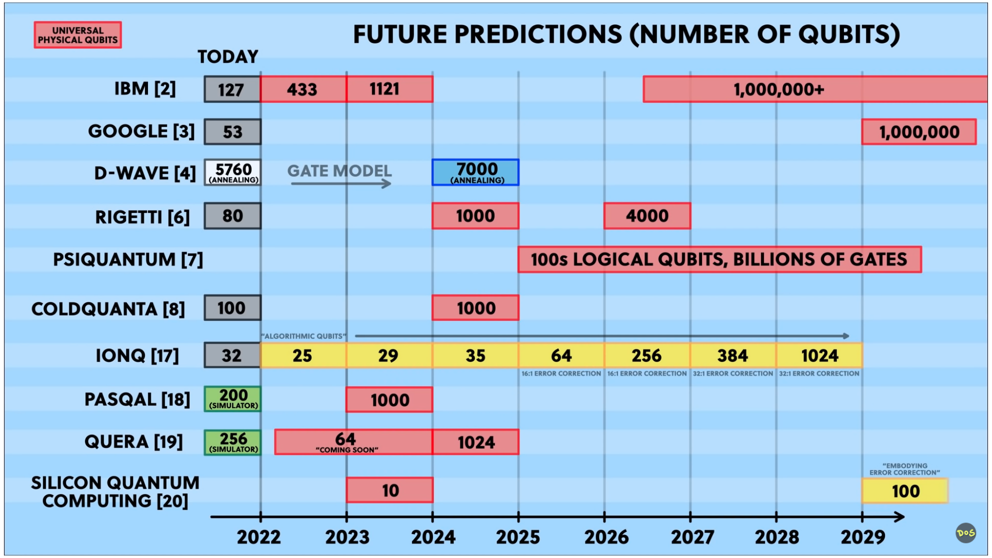

Copyright: D. Walliman. The Map of Quantum Computing, 2022.

Copyright: Forschungszentrum Jülich / Sascha Kreklau

- QC are steadily improving
- How can computer vision benefit from QC?

From a Classical to a Quantum Perspective

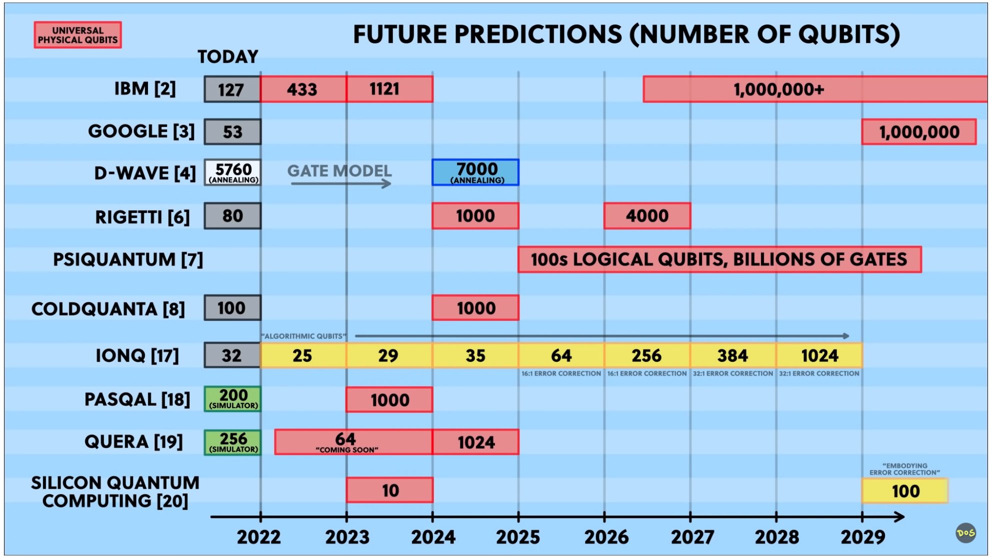

Copyright: D. Walliman. The Map of Quantum Computing, 2022.

Copyright: Forschungszentrum Jülich / JUNIQ

- QC are steadily improving
- How can computer vision benefit from QC?

max planck institut informatik

Foundations of Adiabatic Quantum Computing (AQC)

Quantum annealing in the transverse Ising model

Tadashi Kadowaki and Hidetoshi Nishimori
Department of Physics, Tokyo Institute of Technology, Oh-okayama, Meguro-ku, Tokyo 152-8551, Japan
(Received 30 April 1998)

We introduce quantum fluctuations into the simulated annealing process of optimization problems, aiming at faster convergence to the optimal state. Quantum fluctuations cause transitions between states and thus play the same role as thermal fluctuations in the conventional approach. The idea is tested by the transverse Ising model, in which the transverse field is a function of time similar to the temperature in the conventional method. The goal is to find the ground state of the diagonal part of the Hamiltonian with high accuracy as quickly as possible. We have solved the time-dependent Schrödinger equation numerically for small size systems with various exchange interactions. Comparison with the results of the corresponding classical (thermal) method reveals that the quantum annealing leads to the ground state with much larger probability in almost all cases if we use the same annealing schedule. [S1063-651X(98)02910-9]

Kadowaki and Nishimori, 1998

REPORTS

A Quantum Adiabatic Evolution Algorithm Applied to Random Instances of an NP-Complete Problem

Edward Farhi,[1*] Jeffrey Goldstone,[1] Sam Gutmann,[2] Joshua Lapan,[3] Andrew Lundgren,[3] Daniel Preda[3]

A quantum system will stay near its instantaneous ground state if the Hamiltonian that governs its evolution varies slowly enough. This quantum adiabatic behavior is the basis of a new class of algorithms for quantum computing. We tested one such algorithm by applying it to randomly generated hard instances of an NP-complete problem. For the small examples that we could simulate, the quantum adiabatic algorithm worked well, providing evidence that quantum computers (if large ones can be built) may be able to outperform ordinary computers on hard sets of instances of NP-complete problems.

Although a large quantum computer has yet to be built, the rules for programming such a device, which are derived from the laws of quantum mechanics, are well established. It is already known that quantum computers could solve problems believed to be intractable on classical (i.e., nonquantum) computers. An intractable problem is one that necessarily takes too long to solve when the input gets too big. More precisely, a classically intractable problem is one that cannot be solved using any classical algorithm whose running time grows only polynomially as a function of the length of the input. For example, all known classical factoring algorithms require a time that grows faster than any polynomial as a function of the number of digits in the integer to be factored. Shor's quantum algorithm for the factoring problem (*1*) can factor an integer in a time that grows (roughly) as the square of the number of digits. This raises the question of whether quantum computers could solve other classically difficult prob-

[1]Center for Theoretical Physics, Massachusetts Institute of Technology, Cambridge, MA 02139, USA. [2]Department of Mathematics, Northeastern University, Boston, MA 02115, USA. [3]Massachusetts Institute of Technology, Cambridge, MA 02139, USA.

*To whom correspondence should be addressed. E-mail: farhi@mit.edu

Farhi et al., 2001

Kadowaki and Nishimori. Quantum Annealing in the Transverse Ising Model. Phys. Rev. E, 1998.
Farhi et al. Quantum Adiabatic Evolution Algorithm Applied to Random Instances of an NP-Complete Problem. Science, 2001.

Foundations of AQC (D-Wave)

Initial state: $$|\psi(t=0)\rangle = \bigotimes_{i=1}^{n} \frac{1}{\sqrt{2}}\left(|0\rangle + |1\rangle\right)$$

Transition (simplified): $$H(t) = \left(1 - \frac{t}{\tau}\right) H_I + \frac{t}{\tau} H_P$$

Final state encoding the problem and the data:

$$\boxed{\min_{s \in \{-1,1\}^n} \; s^\top J s + b^\top s}$$

binary vector (qubits during optimisation) | **qubit couplings (interaction weights)** | **qubit biases (individual weights)**

Exemplary Q (QUBO, 21 qubits):

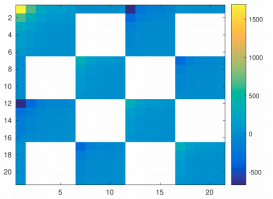

Quadratic Unconstrained Binary Optimisation (QUBO) problem:

$$\arg\min_{\mathbf{x} \in \mathcal{B}^n} \mathbf{x}^\top \mathbf{Q} \mathbf{x} + \mathbf{s}^\top \mathbf{x}$$

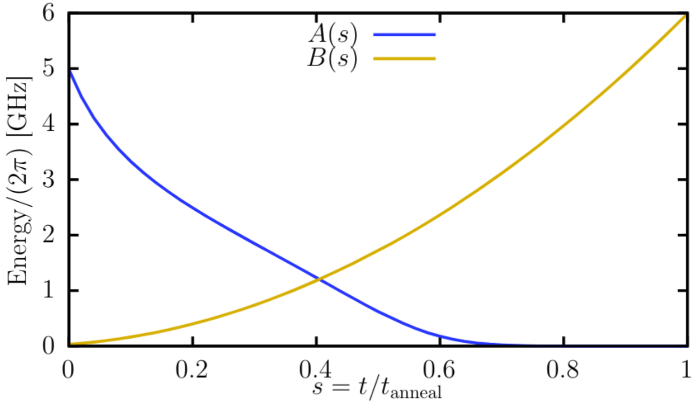

Image: Willsch et al. Computer Physics Communications, 2022.

Annealing functions (schedules)

max planck institut informatik

Farhi et al. Quantum Adiabatic Evolution Algorithm Applied to Random Instances of an NP-Complete Problem. Science, 2001.

Five Steps of Every AQC Algorithm

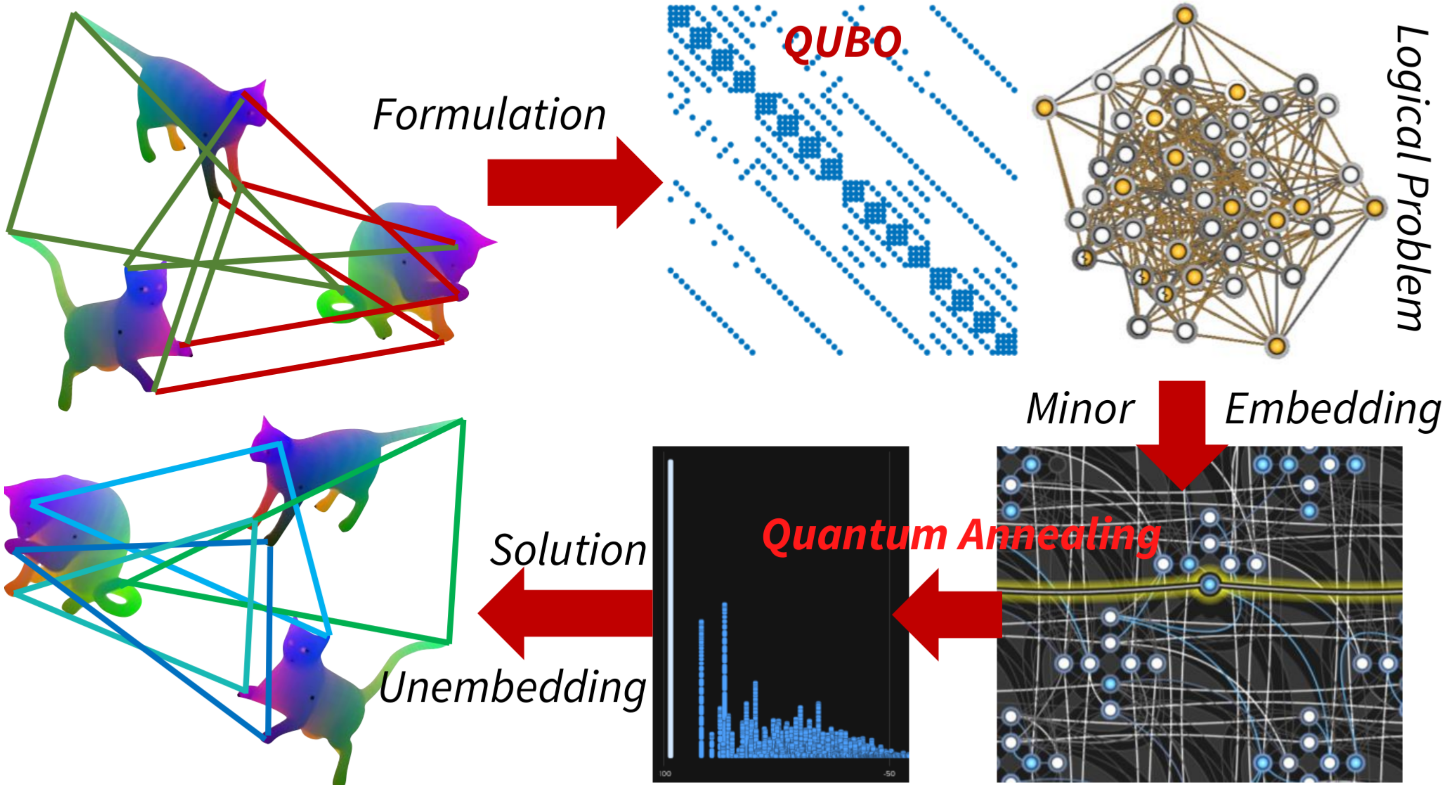

Image: Birdal and Golyanik et al., CVPR 2021.

Five Steps of Every AQC Algorithm

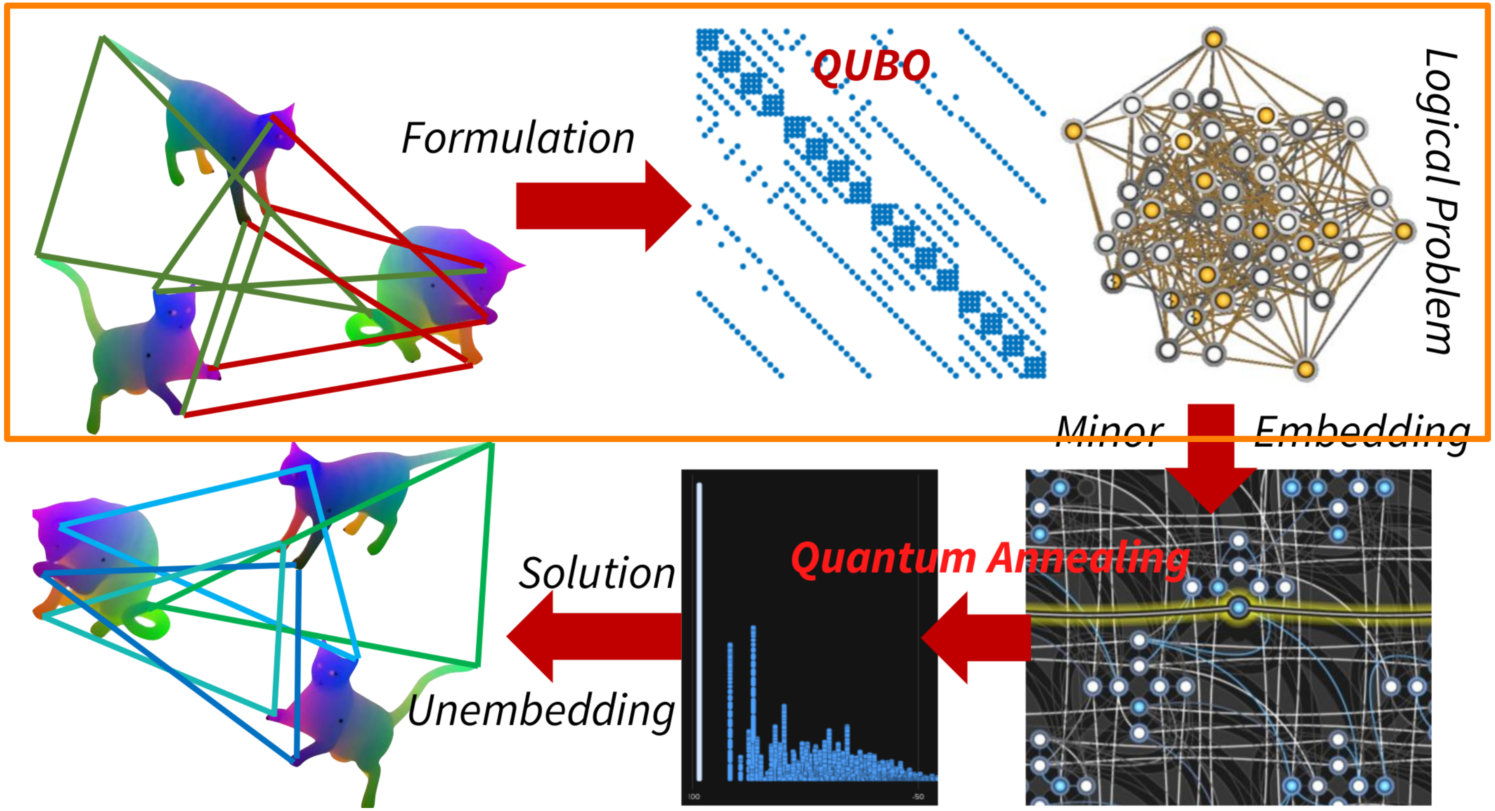

Image: Birdal and Golyanik et al., CVPR 2021.

D-Wave Quantum Annealers

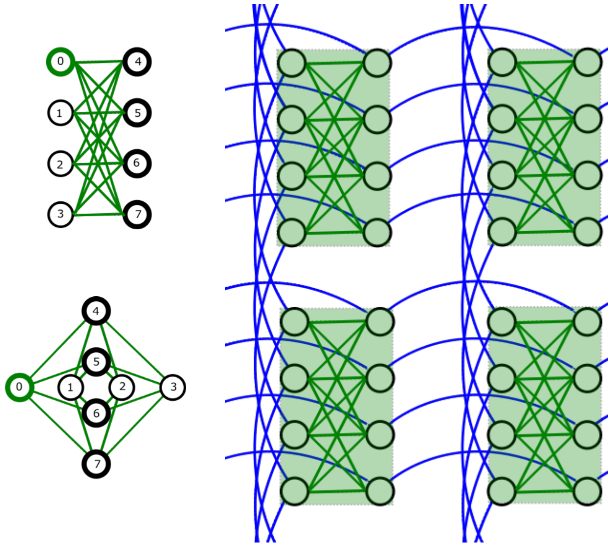

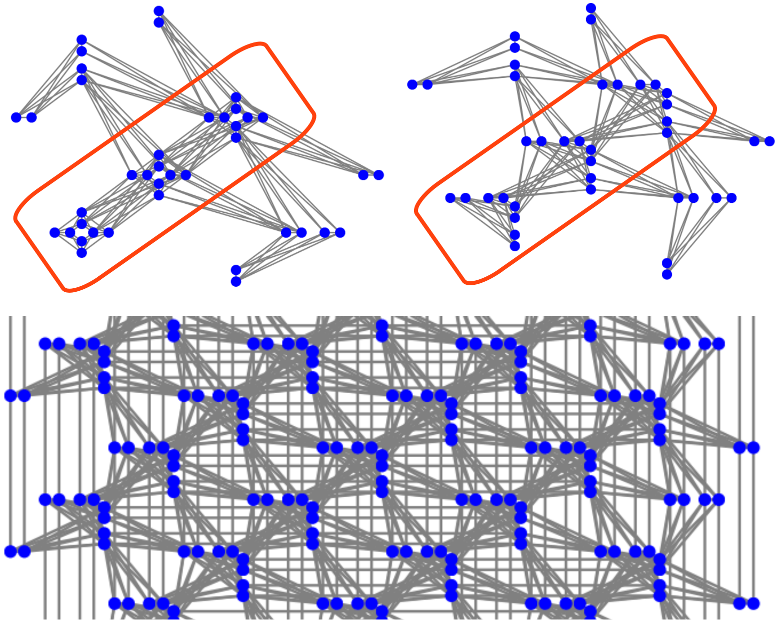

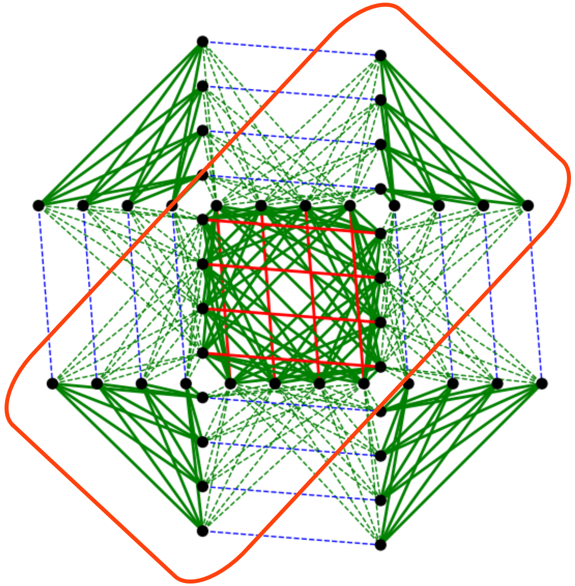

- 2048 qubits (16x16x8)
- Nominal length 4 (internal couplers)
- Degree 6 (+2 external qubits)
- Internal and external couplers

2000Q

- 5640 qubits (~16x16x24)
- Nominal length 12 (internal couplers)
- Degree 15 (+3 external qubits)
- Internal, external and odd couplers

Advantage

- 7440 qubits (~15x15x32)
- Nominal length 16 (internal couplers)
- Degree 20 (+4 external qubits)
- Internal, external and odd couplers

Advantage 2

Images: Silva et al., QIP, 2021; Dwave. D-Wave QPU Architecture: Topologies.

Permutation Synchronisation

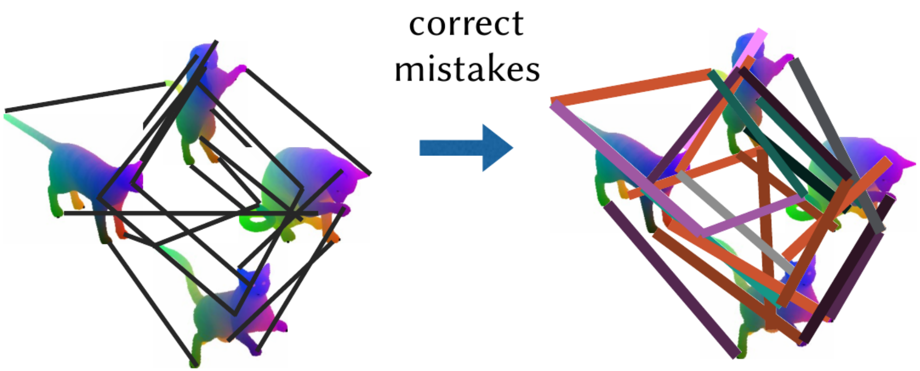

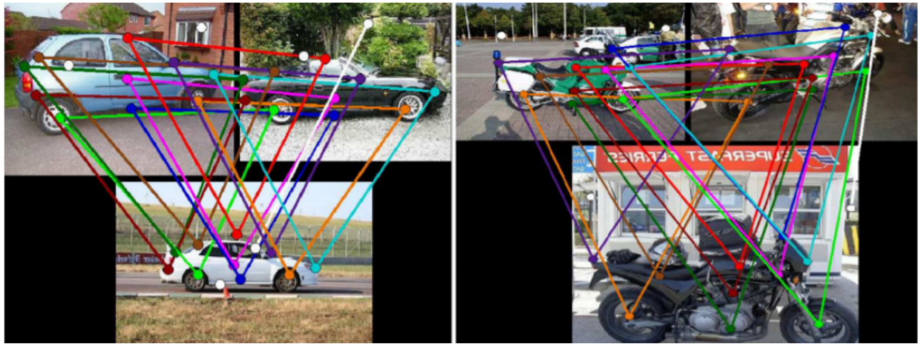

2D or 3D inputs

Birdal and Golyanik et al., CVPR 2021.

Permutation Synchronisation

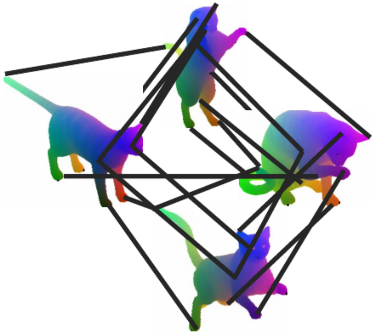

correct
mistakes

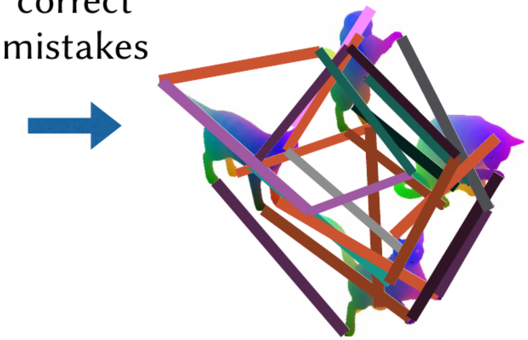

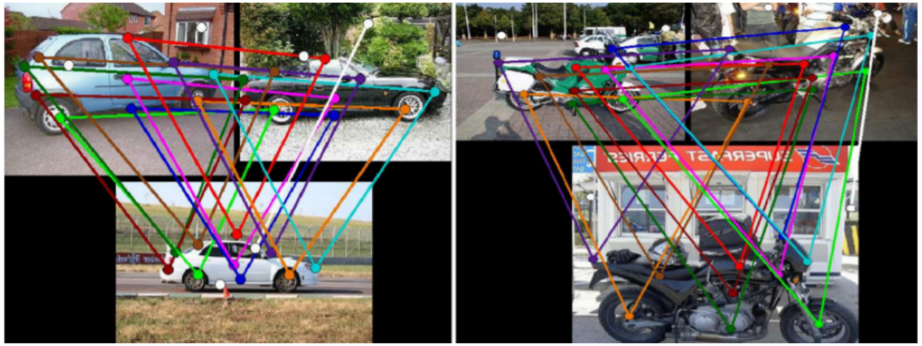

2D or 3D inputs

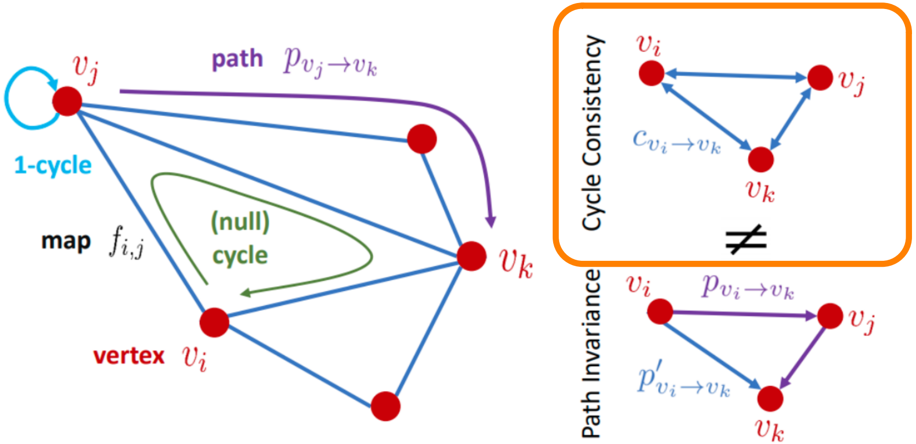

Birdal and Golyanik et al., CVPR 2021.

Permutation Synchronisation

$$\underset{\{\mathbf{X}_i \in \mathcal{P}_n\}}{\arg\min} \sum_{(i,j)\in\mathcal{E}} \|\mathbf{P}_{ij} - \mathbf{X}_i\mathbf{X}_j^\top\|_\mathrm{F}^2 = \underset{\{\mathbf{X}_i \in \mathcal{P}_n\}}{\arg\min}\ \mathbf{x}^\top\mathbf{Q}'\mathbf{x},$$

$$\mathbf{Q}' = -\begin{bmatrix} \mathbf{I}\otimes\mathbf{P}_{11} & \mathbf{I}\otimes\mathbf{P}_{12} & \cdots & \mathbf{I}\otimes\mathbf{P}_{1m} \\ \mathbf{I}\otimes\mathbf{P}_{21} & \mathbf{I}\otimes\mathbf{P}_{22} & \cdots & \mathbf{I}\otimes\mathbf{P}_{2m} \\ \vdots & \vdots & \ddots & \vdots \\ \mathbf{I}\otimes\mathbf{P}_{m1} & \mathbf{I}\otimes\mathbf{P}_{m2} & \cdots & \mathbf{I}\otimes\mathbf{P}_{mm} \end{bmatrix}.$$

max planck institut informatik

Birdal and Golyanik et al., CVPR 2021.

Permutation Synchronisation

$$\arg\min_{\{\mathbf{X}_i \in \mathcal{P}_n\}} \sum_{(i,j)\in\mathcal{E}} \|\mathbf{P}_{ij} - \mathbf{X}_i\mathbf{X}_j^\top\|_\mathrm{F}^2 = \arg\min_{\{\mathbf{X}_i \in \mathcal{P}_n\}} \mathbf{x}^\top \mathbf{Q}' \mathbf{x},$$

$$\mathbf{Q}' = -\begin{bmatrix} \mathbf{I}\otimes\mathbf{P}_{11} & \mathbf{I}\otimes\mathbf{P}_{12} & \cdots & \mathbf{I}\otimes\mathbf{P}_{1m} \\ \mathbf{I}\otimes\mathbf{P}_{21} & \mathbf{I}\otimes\mathbf{P}_{22} & \cdots & \mathbf{I}\otimes\mathbf{P}_{2m} \\ \vdots & \vdots & \ddots & \vdots \\ \mathbf{I}\otimes\mathbf{P}_{m1} & \mathbf{I}\otimes\mathbf{P}_{m2} & \cdots & \mathbf{I}\otimes\mathbf{P}_{mm} \end{bmatrix}.$$

$$\arg\min_{\mathbf{x}\in\mathcal{B}} \mathbf{x}^\top \mathbf{Q}' \mathbf{x} \quad s.t. \quad \mathbf{A}\mathbf{x} = \mathbf{b}$$

is turned into

$$\arg\min_{\mathbf{x}\in\mathcal{B}} \mathbf{x}^\top \mathbf{Q}\mathbf{x} + \mathbf{s}^\top \mathbf{x},$$

where $\boxed{\mathbf{Q} = \mathbf{Q}' + \lambda\mathbf{A}^\top\mathbf{A}}$ *and* $\mathbf{s} = \boxed{-2\lambda\mathbf{A}^\top\mathbf{b}.}$

Birdal and Golyanik et al., CVPR 2021.

Permutation Synchronisation

$$\underset{\{\mathbf{X}_i \in \mathcal{P}_n\}}{\arg\min} \sum_{(i,j)\in\mathcal{E}} \|\mathbf{P}_{ij} - \mathbf{X}_i \mathbf{X}_j^\top\|_F^2 = \underset{\{\mathbf{X}_i \in \mathcal{P}_n\}}{\arg\min}\ \mathbf{x}^\top \mathbf{Q}' \mathbf{x},$$

$$\mathbf{Q}' = -\begin{bmatrix} \mathbf{I}\otimes\mathbf{P}_{11} & \mathbf{I}\otimes\mathbf{P}_{12} & \cdots & \mathbf{I}\otimes\mathbf{P}_{1m} \\ \mathbf{I}\otimes\mathbf{P}_{21} & \mathbf{I}\otimes\mathbf{P}_{22} & \cdots & \mathbf{I}\otimes\mathbf{P}_{2m} \\ \vdots & \vdots & \ddots & \vdots \\ \mathbf{I}\otimes\mathbf{P}_{m1} & \mathbf{I}\otimes\mathbf{P}_{m2} & \cdots & \mathbf{I}\otimes\mathbf{P}_{mm} \end{bmatrix}.$$

$$\underset{\mathbf{x}\in\mathcal{B}}{\arg\min}\ \mathbf{x}^\top \mathbf{Q}' \mathbf{x} \quad s.t. \quad \mathbf{A}\mathbf{x} = \mathbf{b}$$

is turned into

$$\underset{\mathbf{x}\in\mathcal{B}}{\arg\min}\ \mathbf{x}^\top \mathbf{Q}\mathbf{x} + \mathbf{s}^\top \mathbf{x},$$

where $\boxed{\mathbf{Q} = \mathbf{Q}' + \lambda \mathbf{A}^\top \mathbf{A}}$ *and* $\mathbf{s} = \boxed{-2\lambda\mathbf{A}^\top \mathbf{b}.}$

$$\mathcal{P}_n := \{\underbrace{\mathbf{P} \in \{0,1\}^{n\times n}}_{\text{Binary}} : \underbrace{\mathbf{P}\mathbf{1}_n = \mathbf{1}_n}_{\text{Rows sum to 1}},\ \underbrace{\mathbf{1}_n^\top \mathbf{P} = \mathbf{1}_n^\top}_{\text{Cols sum to 1}}\}$$

$$\mathbf{A}_i = \begin{bmatrix} \mathbf{I}\otimes\mathbf{1}^\top \\ \mathbf{1}^\top \otimes \mathbf{I} \end{bmatrix} \quad \Rightarrow \quad \mathbf{A} = \begin{bmatrix} \mathbf{A}_1 & & & \\ & \mathbf{A}_2 & & \\ & & \ddots & \\ & & & \mathbf{A}_n \end{bmatrix}$$

$$\mathbf{b}_i = \mathbf{1} \qquad \mathbf{b} = \mathbf{1}$$

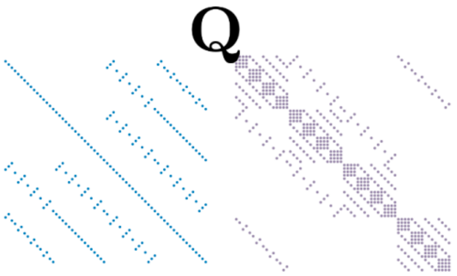

unconstrained constrained

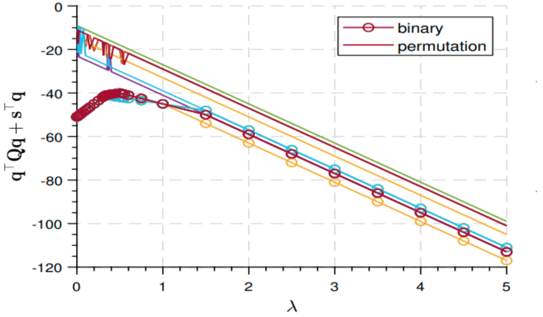

Birdal and Golyanik et al., CVPR 2021.

max planck institut
informatik

Permutation Synchronisation

	Car	Duck	Motorbike	Winebottle	Average
Exhaustive	**0.84 ± 0.104**	**0.91 ± 0.115**	**0.82 ± 0.10**	**0.95 ± 0.096**	**0.88 ± 0.104**
EIG	0.81 ± 0.083	0.86 ± 0.102	0.77 ± 0.059	0.87 ± 0.107	0.83 ± 0.088
ALS	**0.84 ± 0.095**	0.90 ± 0.102	0.81 ± 0.078	0.94 ± 0.092	0.87 ± 0.092
LIFT	**0.84 ± 0.102**	0.90 ± 0.103	0.81 ± 0.078	0.94 ± 0.092	0.87 ± 0.094
Birkhoff	**0.84 ± 0.094**	0.90 ± 0.107	0.81 ± 0.079	0.94 ± 0.093	0.87 ± 0.093
D-Wave(Ours)	**0.84 ± 0.104**	0.90 ± 0.104	0.81 ± 0.080	0.93 ± 0.095	0.87 ± 0.096

Average Errors

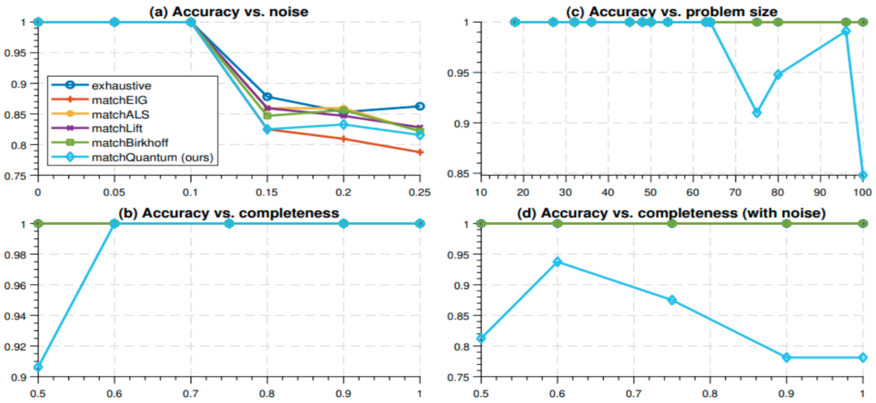

Evaluations on the synthetic dataset (4 views and 4 points)

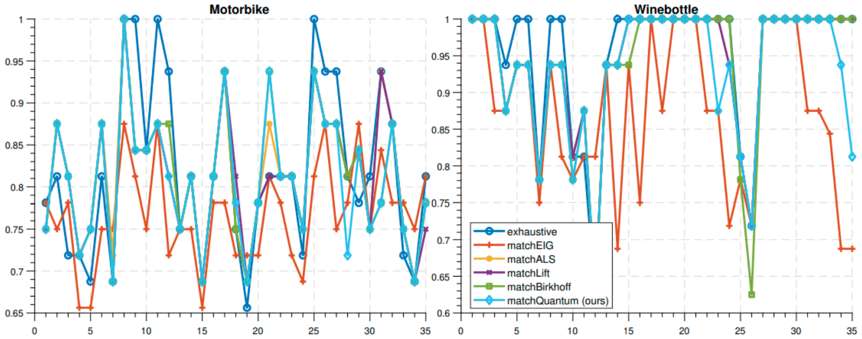

Detailed evaluations over all the subsets

Birdal and Golyanik et al., CVPR 2021.

Permutation Synchronisation

	Car	Duck	Motorbike	Winebottle	Average
Exhaustive	**0.84 ± 0.104**	**0.91 ± 0.115**	**0.82 ± 0.10**	**0.95 ± 0.096**	**0.88 ± 0.104**
EIG	0.81 ± 0.083	0.86 ± 0.102	0.77 ± 0.059	0.87 ± 0.107	0.83 ± 0.088
ALS	**0.84 ± 0.095**	0.90 ± 0.102	0.81 ± 0.078	0.94 ± 0.092	0.87 ± 0.092
LIFT	**0.84 ± 0.102**	0.90 ± 0.103	0.81 ± 0.078	0.94 ± 0.092	0.87 ± 0.094
Birkhoff	**0.84 ± 0.094**	0.90 ± 0.107	0.81 ± 0.079	0.94 ± 0.093	0.87 ± 0.093
D-Wave(Ours)	**0.84 ± 0.104**	0.90 ± 0.104	0.81 ± 0.080	0.93 ± 0.095	0.87 ± 0.096

Average Errors

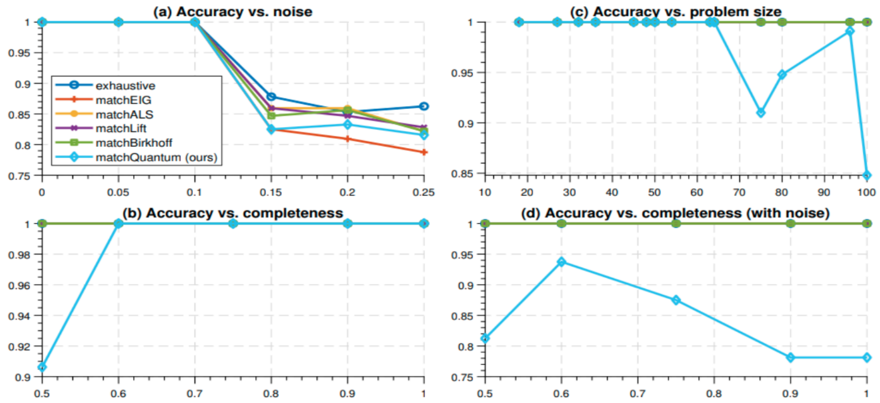

Evaluations on the synthetic dataset (4 views and 4 points)

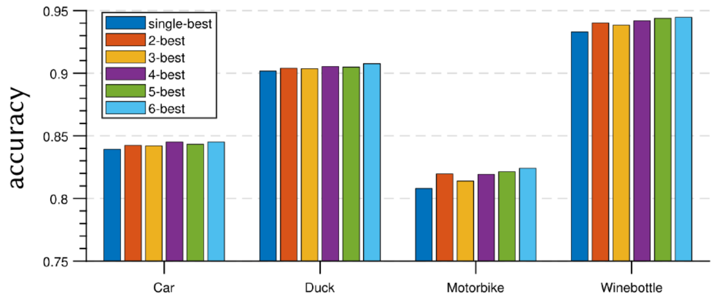

Bit corrections using multiple measurements of different energies

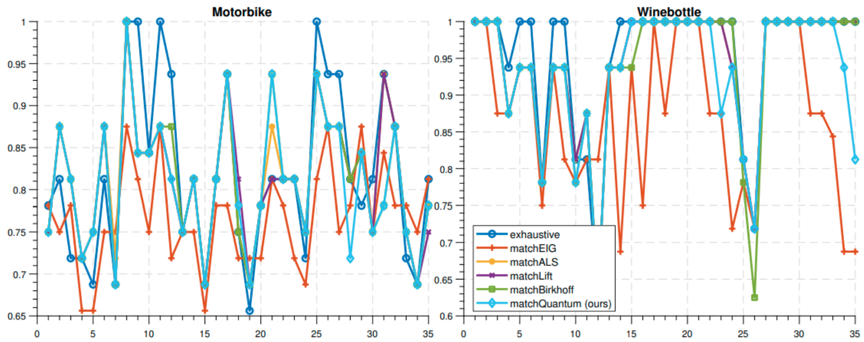

Detailed evaluations over all the subsets

max planck institut informatik

Birdal and Golyanik et al., CVPR 2021.

Permutation Synchronisation

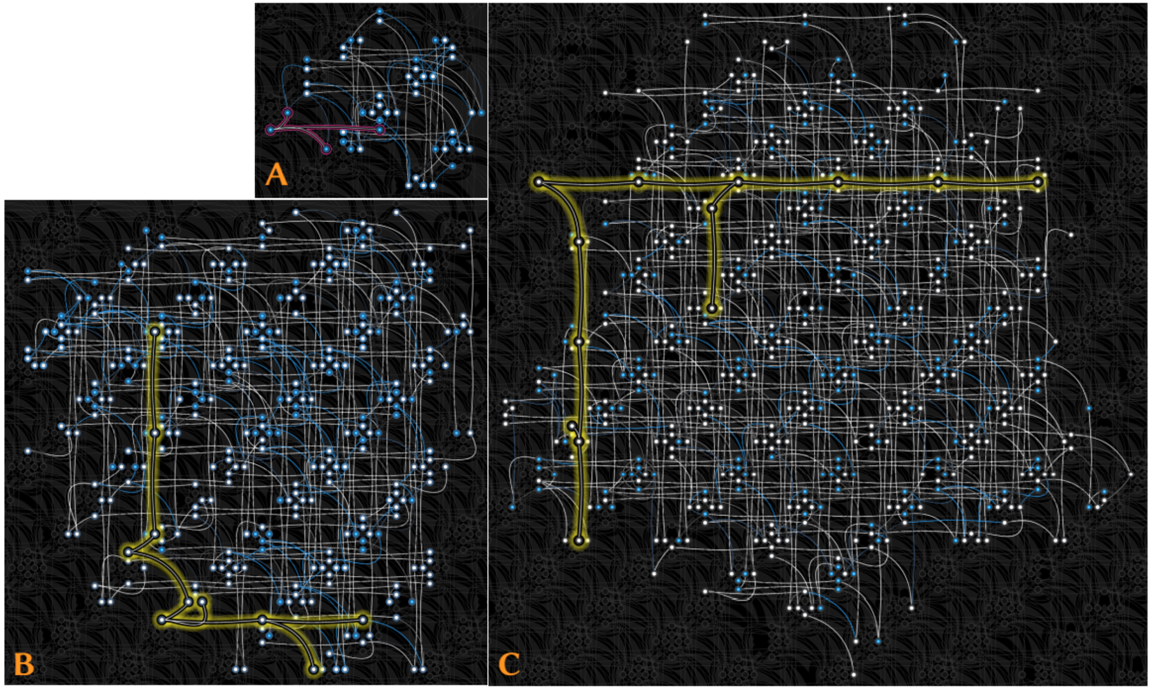

Exemplary minor embeddings in the experiments with
- n = 3, m = 3 (A, N = 49),
- n = 4, m = 4 (B, N = 341), and
- n = 3, m = 8 (C, N = 550).

max planck institut informatik

Birdal and Golyanik et al., CVPR 2021.

Permutation Synchronisation

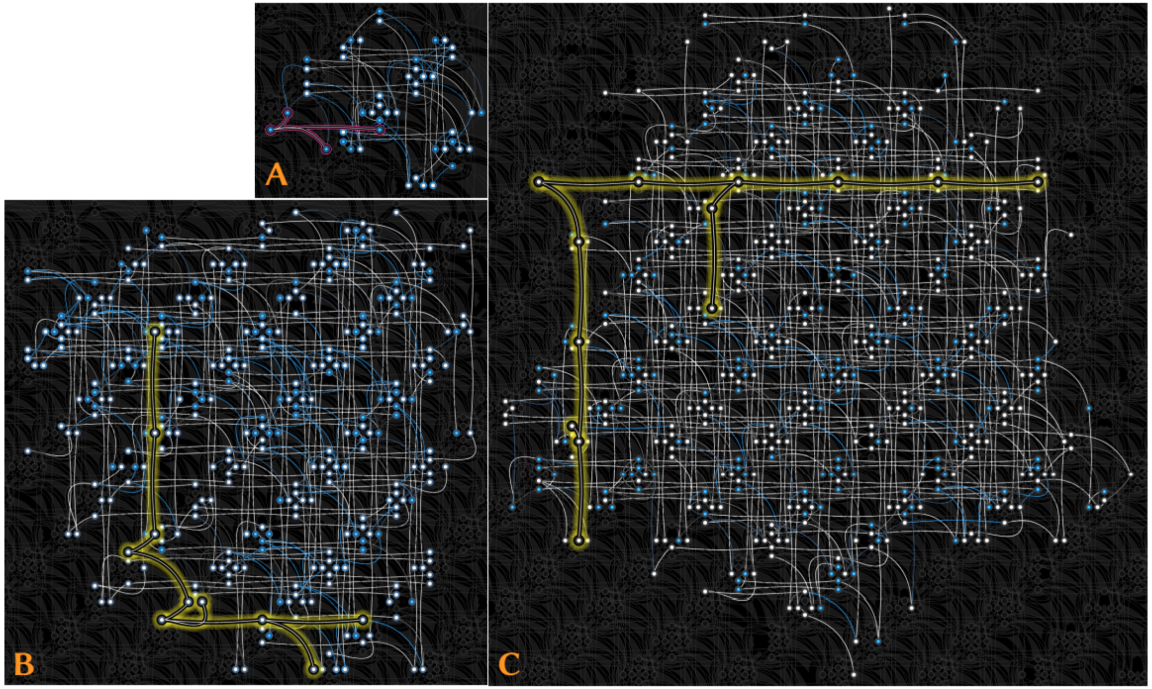

Exemplary minor embeddings in the experiments with
- n = 3, m = 3 (A, N = 49),
- n = 4, m = 4 (B, N = 341), and
- n = 3, m = 8 (C, N = 550).

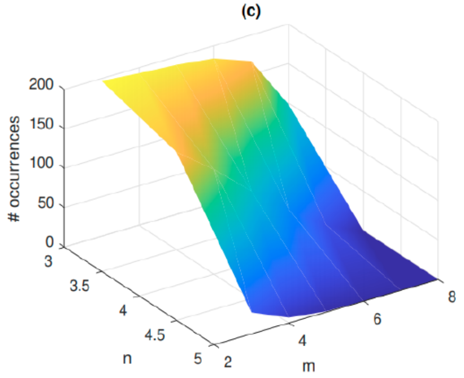

Average number of measured optimal solutions

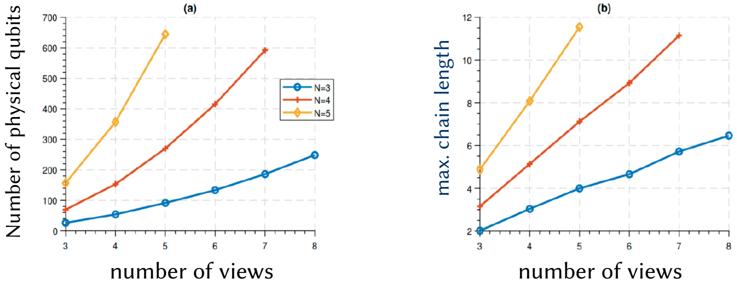

Minor embedding functions

Birdal and Golyanik et al., CVPR 2021.

max planck institut informatik

Motion Segmentation

$$\boxed{Z_{ij} = X_i X_j^\top}$$

Goal: Classify points in multiple images into different motions

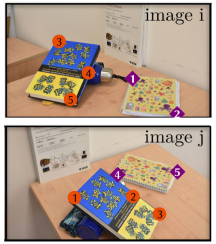

$$\text{image i}\ \begin{array}{c|c} & \text{image j} \\ & 1 \quad 2 \quad 3 \quad 4 \quad 5 \\ \begin{array}{c}1\\2\\3\\4\\5\end{array} & \begin{bmatrix} 0 & 0 & 0 & 1 & 1 \\ 0 & 0 & 0 & 1 & 1 \\ 1 & 1 & 1 & 0 & 0 \\ 1 & 1 & 1 & 0 & 0 \\ 1 & 1 & 1 & 0 & 0 \end{bmatrix} \end{array} \qquad \text{image i}\ \begin{array}{c|c} & \text{motions} \\ \begin{array}{c}1\\2\\3\\4\\5\end{array} & \begin{bmatrix} 0 & 1 \\ 0 & 1 \\ 1 & 0 \\ 1 & 0 \\ 1 & 0 \end{bmatrix} \end{array} \qquad \text{image j}\ \begin{array}{c|c} & \text{motions} \\ \begin{array}{c}1\\2\\3\\4\\5\end{array} & \begin{bmatrix} 1 & 0 \\ 1 & 0 \\ 1 & 0 \\ 0 & 1 \\ 0 & 1 \end{bmatrix} \end{array}$$

Zij — Xi — Xj

two-frame matches (known) — absolute segmentations (unknown)

Arrigoni et al., ECCV 2022.

Motion Segmentation

$$\boxed{Z_{ij} = X_i X_j^\mathsf{T}}$$

Goal: Classify points in multiple images into different motions

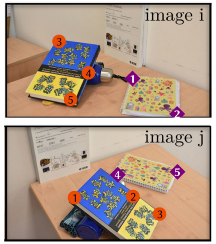

$$\text{image i}\quad \begin{array}{c|c} & \text{image j} \\ & 1\ \ 2\ \ 3\ \ 4\ \ 5 \\ \begin{matrix}1\\2\\3\\4\\5\end{matrix} & \begin{bmatrix}0&0&0&1&1\\0&0&0&1&1\\1&1&1&0&0\\1&1&1&0&0\\1&1&1&0&0\end{bmatrix}\end{array} \qquad \text{image i}\quad \begin{array}{cc} & \text{motions} \\ \begin{matrix}1\\2\\3\\4\\5\end{matrix} & \begin{bmatrix}0&1\\0&1\\1&0\\1&0\\1&0\end{bmatrix}\end{array} \qquad \text{image j}\quad \begin{array}{cc} & \text{motions} \\ \begin{matrix}1\\2\\3\\4\\5\end{matrix} & \begin{bmatrix}1&0\\1&0\\1&0\\0&1\\0&1\end{bmatrix}\end{array}$$

Zij Xi Xj

two-frame matches (known)

absolute segmentations (unknown)

$$\min_{X_1,\ldots X_n} \sum_{(i,j)\in\mathcal{E}} ||Z_{ij} - X_i X_j^\mathsf{T}||_F^2,$$

$$\text{s.t.}\ \ \mathrm{vec}(X_i) \in \mathcal{B}^{p_i}, \quad X_i \mathbf{1}_d = \mathbf{1}_{pi} \quad \forall i = 1,\ldots,n$$

$$X = \begin{bmatrix} X_1 \\ X_2 \\ \ldots \\ X_n \end{bmatrix}, \quad Z = \begin{bmatrix} 0 & Z_{12} & \ldots & Z_{1n} \\ Z_{21} & 0 & \ldots & Z_{2n} \\ \ldots & & & \ldots \\ Z_{n1} & Z_{n2} & \ldots & 0 \end{bmatrix}$$

Arrigoni et al., ECCV 2022.

Motion Segmentation

$$\boxed{Z_{ij} = X_i X_j^{\mathsf{T}}}$$

Goal: Classify points in multiple images into different motions

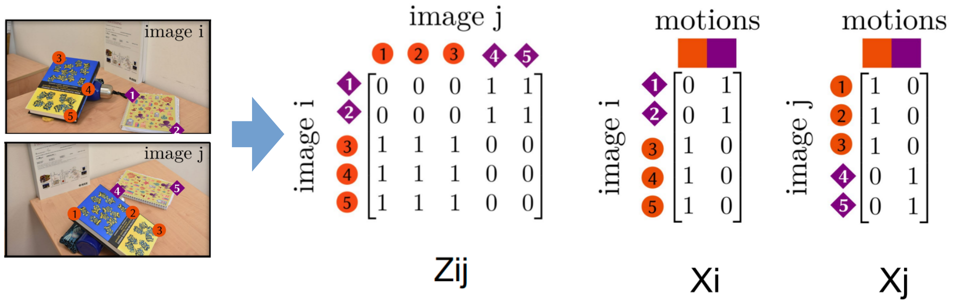

two-frame matches (known)

absolute segmentations (unknown)

$$\min_{X_1,\ldots X_n} \sum_{(i,j)\in\mathcal{E}} ||Z_{ij} - X_i X_j^{\mathsf{T}}||_F^2,$$

$$\text{s.t.} \;\; \mathrm{vec}(X_i) \in \mathcal{B}^{p_i}, \quad X_i \mathbf{1}_d = \mathbf{1}_{pi} \quad \forall i = 1, \ldots, n$$

$$X = \begin{bmatrix} X_1 \\ X_2 \\ \ldots \\ X_n \end{bmatrix}, \quad Z = \begin{bmatrix} 0 & Z_{12} & \ldots & Z_{1n} \\ Z_{21} & 0 & \ldots & Z_{2n} \\ \ldots & & & \ldots \\ Z_{n1} & Z_{n2} & \ldots & 0 \end{bmatrix}$$

?

$$\min_{\mathbf{y}\in\mathcal{B}^k} \mathbf{y}^{\mathsf{T}} Q \mathbf{y} + \mathbf{s}^{\mathsf{T}} \mathbf{y} + \sum_i \lambda_i \, ||A_i \mathbf{y} - \mathbf{b_i}||^2$$

Arrigoni et al., ECCV 2022.

Permutation Synchronisation

$$\min_{X_1,\dots X_n} \sum_{(i,j)\in\mathcal{E}} ||Z_{ij} - X_i X_j^{\mathsf{T}}||_F^2,$$

$$\text{s.t. } \operatorname{vec}(X_i) \in \mathcal{B}^{p_i}, \quad X_i \mathbf{1}_d = \mathbf{1}_{pi} \quad \forall i = 1,\dots,n$$

binary variables   each point belongs to one motion

$$X = \begin{bmatrix} X_1 \\ X_2 \\ \dots \\ X_n \end{bmatrix}, \quad Z = \begin{bmatrix} 0 & Z_{12} & \dots & Z_{1n} \\ Z_{21} & 0 & \dots & Z_{2n} \\ \dots & & & \dots \\ Z_{n1} & Z_{n2} & \dots & 0 \end{bmatrix}$$

Arrigoni et al., ECCV 2022.

Permutation Synchronisation

$$\min_{X_1,\dots X_n} \sum_{(i,j)\in\mathcal{E}} ||Z_{ij} - X_i X_j^\mathsf{T}||_F^2,$$

$$\text{s.t. } \operatorname{vec}(X_i) \in \mathcal{B}^{p_i}, \quad X_i \mathbf{1}_d = \mathbf{1}_{pi} \quad \forall i = 1,\dots,n$$

<u>binary variables</u> <u>each point belongs to one motion</u>

$$X = \begin{bmatrix} X_1 \\ X_2 \\ \dots \\ X_n \end{bmatrix}, \quad Z = \begin{bmatrix} 0 & Z_{12} & \dots & Z_{1n} \\ Z_{21} & 0 & \dots & Z_{2n} \\ \dots & & & \dots \\ Z_{n1} & Z_{n2} & \dots & 0 \end{bmatrix}$$

QuMoSeg-v1, dense Q

$$\max_{X_1,\dots X_n} \sum_{(i,j)\in\mathcal{E}} \operatorname{trace}(X_i^\mathsf{T}(2Z_{ij} - \mathbf{1}_{p_i\times p_j})X_j)$$

$$s.t. \ \operatorname{vec}(X_i) \in \mathcal{B}^{p_i}, \quad X_i \mathbf{1}_d = \mathbf{1}_{pi} \quad \forall i = 1,\dots,n$$

$$\downarrow$$

$$\max_X \operatorname{vec}(X)^\mathsf{T}(I_{d\times d} \otimes (2Z - \mathbf{1}_{p\times p}))\operatorname{vec}(X),$$

$$s.t. \ \operatorname{vec}(X) \in \mathcal{B}^{dp}, \quad X\mathbf{1}_d = \mathbf{1}_p.$$

Arrigoni et al., ECCV 2022.

Permutation Synchronisation

$$\min_{X_1,\dots X_n} \sum_{(i,j)\in\mathcal{E}} \|Z_{ij} - X_i X_j^\mathsf{T}\|_F^2, \qquad X = \begin{bmatrix} X_1 \\ X_2 \\ \dots \\ X_n \end{bmatrix}, \quad Z = \begin{bmatrix} 0 & Z_{12} & \dots & Z_{1n} \\ Z_{21} & 0 & \dots & Z_{2n} \\ \dots & & & \dots \\ Z_{n1} & Z_{n2} & \dots & 0 \end{bmatrix}$$

$$\text{s.t. } \operatorname{vec}(X_i) \in \mathcal{B}^{p_i}, \quad X_i \mathbf{1}_d = \mathbf{1}_{pi} \quad \forall i = 1,\dots,n$$

binary variables — each point belongs to one motion

QuMoSeg-v1, dense Q

$$\max_{X_1,\dots X_n} \sum_{(i,j)\in\mathcal{E}} \operatorname{trace}(X_i^\mathsf{T}(2Z_{ij} - \mathbf{1}_{p_i\times p_j})X_j)$$

$$s.t.\ \operatorname{vec}(X_i) \in \mathcal{B}^{p_i}, \quad X_i\mathbf{1}_d = \mathbf{1}_{pi} \quad \forall i = 1,\dots,n$$

$$\max_X \operatorname{vec}(X)^\mathsf{T}(I_{d\times d} \otimes (2Z - \mathbf{1}_{p\times p}))\operatorname{vec}(X),$$

$$s.t.\ \operatorname{vec}(X) \in \mathcal{B}^{dp}, \quad X\mathbf{1}_d = \mathbf{1}_p.$$

QuMoSeg-v2, sparse Q (additional assumptions)

$$\max_{X_1,\dots X_n} \sum_{(i,j)\in\mathcal{E}} \operatorname{trace}(X_i^\mathsf{T} Z_{ij} X_j),$$

$$s.t.\ \operatorname{vec}(X_i) \in \mathcal{B}^{p_i}, \quad X_i\mathbf{1}_d = \mathbf{1}_{pi}, \quad \mathbf{1}_{p_i}^\mathsf{T} X_i = \mathbf{m}_i^\mathsf{T} \quad \forall i = 1,\dots,n.$$

extra constraints

$$\max_X \operatorname{vec}(X)^\mathsf{T}(I_{d\times d} \otimes Z)\operatorname{vec}(X),$$

$$s.t.\ \operatorname{vec}(X) \in \mathcal{B}^{dp}, \quad X\mathbf{1}_d = \mathbf{1}_p, \quad KX = M$$

Arrigoni et al., ECCV 2022.

Motion Segmentation

$\mu =$ 0.97 0.93 0.93 0.89

ground truth | QuMoSeg | Mode, ICCV'19 | Synch, ICCVW'19 | Xu et al., TPAMI'19

Arrigoni et al., ECCV 2022.

Motion Segmentation

Q-MSEG

# Qubits:	96	102	120	126	128	136	160	168	180	190	200	216	220	243
Xu et al. [63]	0.89	0.89	0.94	0.75	0.96	0.97	0.86	0.86	0.97	0.88	0.96	0.77	0.83	0.74
Mode [5]	0.93	0.93	0.96	0.93	**0.97**	0.97	**0.98**	0.99	**0.98**	**0.99**	**0.99**	0.93	**1**	**0.94**
Synch [4]	0.93	0.94	0.95	0.95	0.84	0.92	0.97	**1**	0.89	0.95	0.90	**0.94**	0.99	0.92
QuMoSeg-v1	0.97	0.97	0.97	0.96	0.95	**0.98**	**0.98**	0.99	**0.98**	**0.99**	**0.99**	0.64	–	–
QuMoSeg-v2	0.96	0.97	0.95	0.94	0.89	0.89	0.88	0.85	0.74	0.75	0.79	0.59	0.75	0.58
QuMoSeg-v1, SA	0.97	0.97	0.97	0.96	0.95	**0.98**	**0.98**	**1**	**0.98**	**0.99**	**0.99**	0.68	0.98	0.72
QuMoSeg-v2, SA	**0.98**	**0.99**	**0.99**	**1**	0.96	**0.98**	**0.98**	**1**	0.94	0.97	**0.99**	0.80	**1**	0.59

Hopkins

# Qubits:	120	126	132	138	144	156	162	168	174	180	186	192	198	204	210	216	222	228	234	240
Xu et al. [63]	0.80	0.78	0.81	0.79	0.83	0.81	0.84	0.81	0.85	0.89	0.88	0.94	0.96	0.96	0.97	**1**	0.98	**1**	**0.99**	**1**
Mode [5]	0.89	0.91	0.90	0.93	0.92	0.94	0.95	0.95	0.96	0.95	0.97	0.98	0.98	0.98	0.98	0.99	0.98	0.98	**0.99**	0.99
Synch [4]	0.87	0.93	0.95	0.96	**0.99**	0.96	**0.99**	**0.99**	0.96	0.99	**1**	**1**	0.99	**1**	**1**	0.70	0.97	**1**	**0.99**	0.65
QuMoSeg-v1	0.92	0.89	0.93	0.93	0.93	0.93	0.95	0.94	0.96	0.95	0.96	0.97	0.96	-	-	-	-	-	-	-
QuMoSeg-v2	0.91	0.92	0.91	0.92	0.94	0.89	0.91	0.89	0.90	0.88	0.88	0.89	0.88	0.89	0.88	-	-	-	-	-
QuMoSeg-v1, SA	0.93	0.90	0.92	0.94	0.93	0.94	0.95	0.96	0.96	0.96	0.98	0.98	0.98	0.98	0.99	0.99	0.98	0.98	**0.99**	0.99
QuMoSeg-v2, SA	**0.96**	**0.97**	**0.98**	**0.98**	**0.99**	**0.99**	**0.99**	0.97	**0.99**	**1**	**1**	**1**	**1**	**1**	**1**	**1**	**0.99**	**1**	**0.99**	**1**

max planck institut informatik

Arrigoni et al., ECCV 2022.

Motion Segmentation

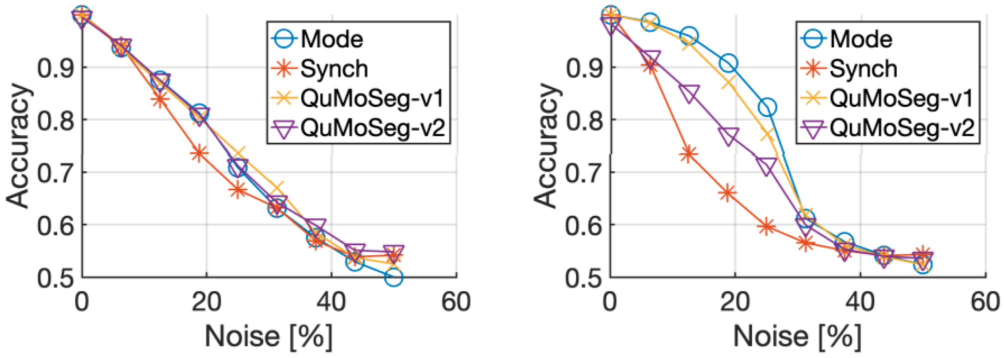

Accuracy under noisy inputs

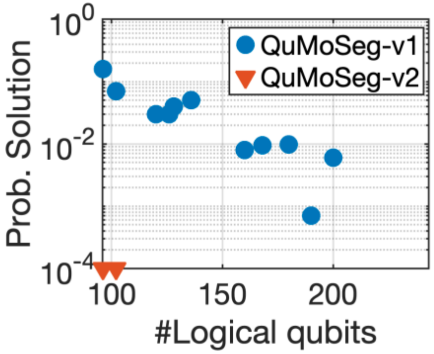

Optimal solution probabilities

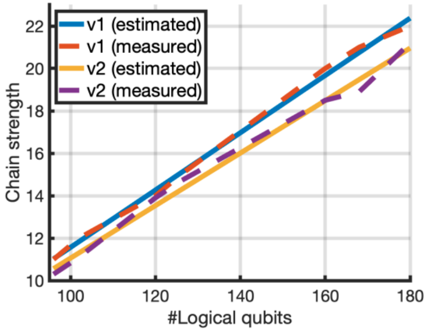

Chain strengths

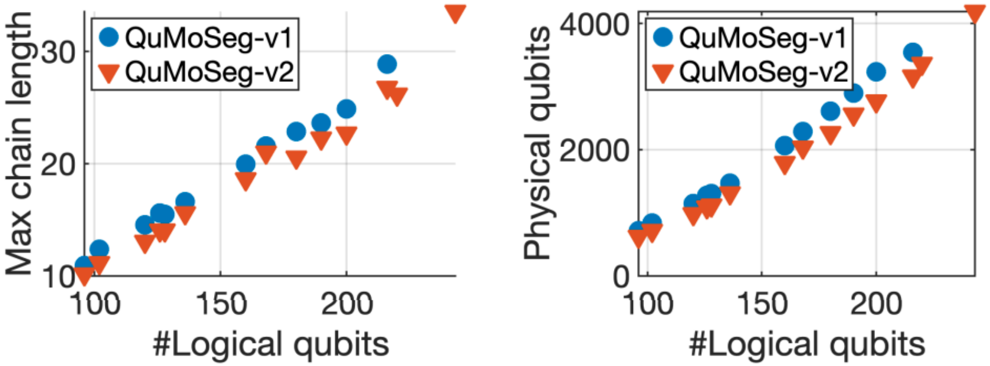

Minor embedding functions

Arrigoni et al., ECCV 2022.

Iterative AQC Algorithms

Iterative AQC Algorithms

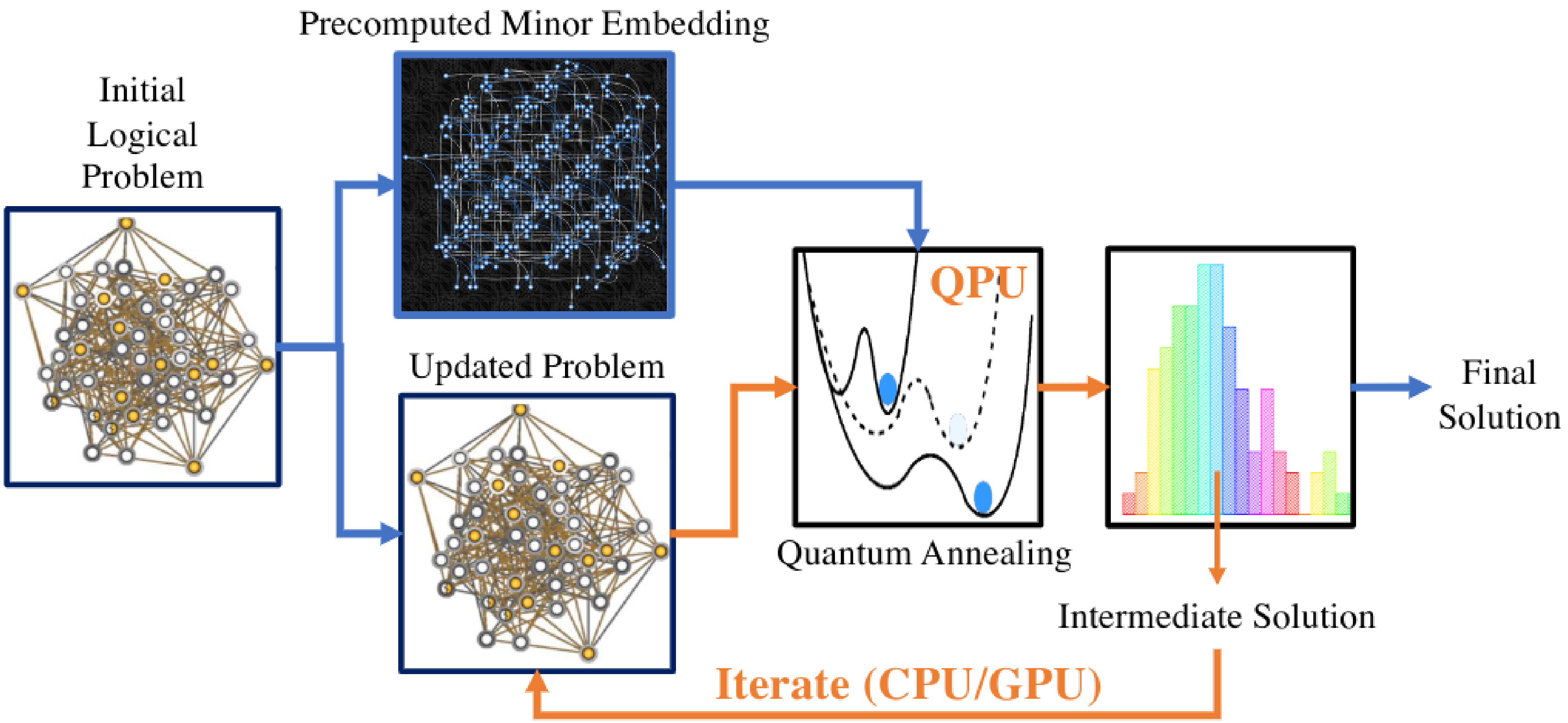

Shape Matching with AQC

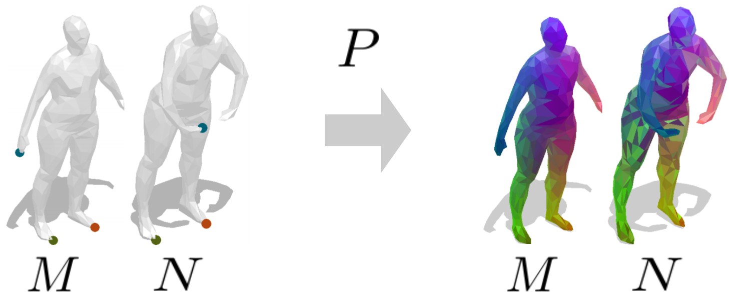

$$\min_{X \in \mathbb{P}_n} \; E(X) := \mathbf{x}^{\mathrm{T}} W \mathbf{x}$$

$$\mathbf{x} \;=\; \mathrm{vec}(X) \qquad W \in \mathbb{R}^{n^2 \times n^2}$$

$\mathbb{P} \;\subset\; \{0,1\}^{n \times n}$ (permutation matrix)

$$\mathbb{P}_n \;=\; \{X \;\in\; \{0,1\}^{n\times n} \mid \textstyle\sum_i X_{ij} \;=\; 1,\; \sum_j X_{ij} \;=\; 1 \;\forall i,j\}.$$

Seelbach Benkner et al., ICCV 2021.

Shape Matching with AQC

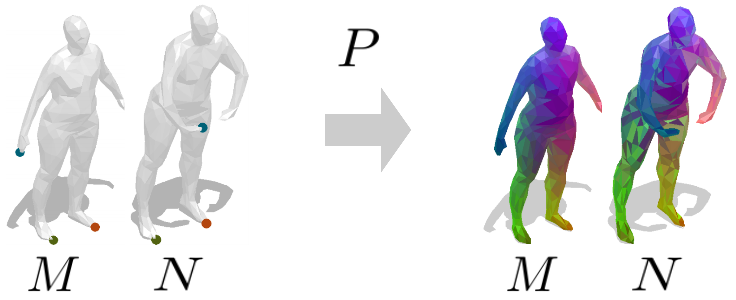

$$\min_{X \in \mathbb{P}_n} \; E(X) := \mathbf{x}^{\mathrm{T}} W \mathbf{x}$$

$$\mathbf{x} \; = \; \mathrm{vec}(X) \qquad W \in \mathbb{R}^{n^2 \times n^2}$$

$$\mathbb{P} \; \subset \; \{0,1\}^{n \times n} \text{ (permutation matrix)}$$

$$\mathbb{P}_n \; = \; \{X \in \{0,1\}^{n \times n} \mid \textstyle\sum_i X_{ij} = 1, \; \sum_j X_{ij} = 1 \; \forall i,j\}.$$

k-cycles:

Disjoint permutations commute:

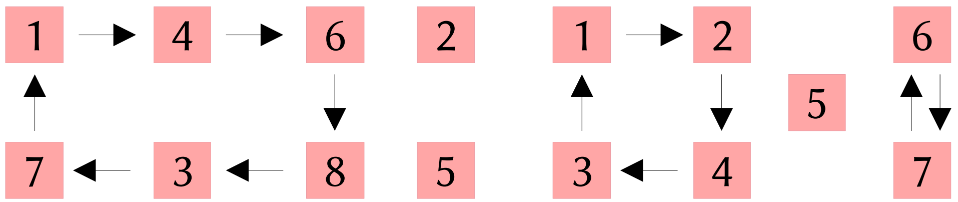

six-cycle   fixed points   four-cycle   two-cycle

Seelbach Benkner et al., ICCV 2021.

Shape Matching with AQC

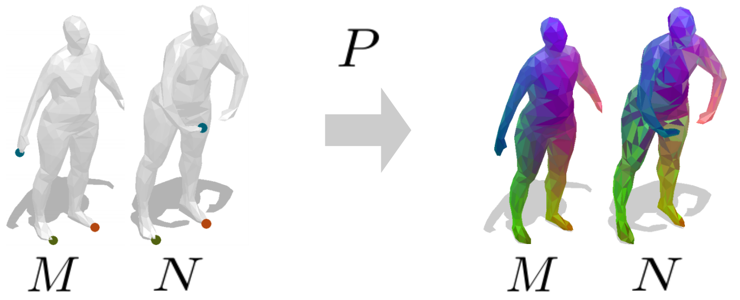

$$\min_{X \in \mathbb{P}_n} \; E(X) := \mathbf{x}^{\mathrm{T}} W \mathbf{x}$$

$$\mathbf{x} \;=\; \mathrm{vec}(X) \qquad W \in \mathbb{R}^{n^2 \times n^2}$$

$$\mathbb{P} \;\subset\; \{0,1\}^{n \times n} \;\; \text{(permutation matrix)}$$

$$\mathbb{P}_n \;=\; \{X \in \{0,1\}^{n \times n} \mid \textstyle\sum_i X_{ij} = 1, \; \sum_j X_{ij} = 1 \;\forall i,j\}.$$

k-cycles:

Disjoint permutations commute:

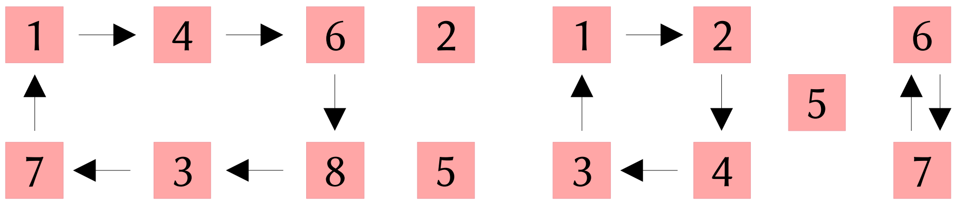

six-cycle   fixed points   four-cycle   two-cycle

Given two cycles C_1, C_2 we parametrize all combinations with two binary variables α_1, α_2

$$\begin{pmatrix} 1-\alpha_1 & 0 & \alpha_1 & 0 & 0 \\ \alpha_1 & 1-\alpha_1 & 0 & 0 & 0 \\ 0 & \alpha_1 & 1-\alpha_1 & 0 & 0 \\ 0 & 0 & 0 & 1-\alpha_2 & \alpha_2 \\ 0 & 0 & 0 & \alpha_2 & 1-\alpha_2 \end{pmatrix}$$

Possible permutations for all choices of α_1, α_2:

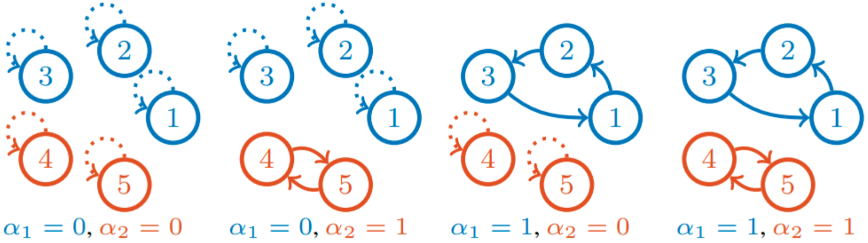

Seelbach Benkner et al., ICCV 2021.

Shape Matching with AQC

Given: 3D shapes M and N, both discretised with n vertices.

$$W_{i \cdot n+k, j \cdot n+l} = |d^g_M(i,j) - d^g_N(k,l)|$$

Find: optimal P

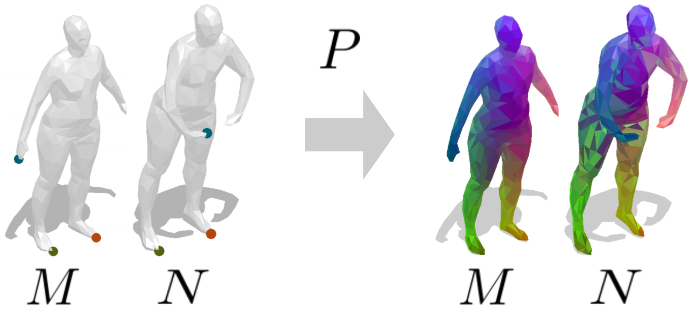

Seelbach Benkner et al., ICCV 2021.

max planck institut informatik

Shape Matching with AQC

Given: 3D shapes M and N, both discretised with n vertices.

$$W_{i\cdot n+k, j\cdot n+l} = |d^g_M(i,j) - d^g_N(k,l)|$$

Find: optimal P

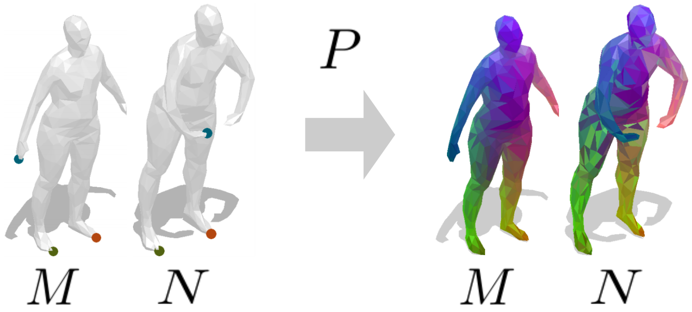

Want to solve but cannot:

$$\min_{X \in \mathbb{P}_n} E(X) := \mathbf{x}^{\mathrm{T}} W \mathbf{x}$$

$$W_{i\cdot n+k, j\cdot n+l} = |d^g_M(i,j) - d^g_N(k,l)|$$

… leading to

not submodular

$$\min_{\alpha \in \{0,1\}^m} \alpha^\top \tilde{W} \alpha \qquad \tilde{W}_{ij} = \begin{cases} E(C_i, C_j) & \text{if } i \neq j, \\ E(C_i, C_i) + E(C_i, P_0) + E(P_0, C_j) & \text{otherwise.} \end{cases}$$

Instead solve

$$\underset{\{P \in \mathbb{P}_n \mid \exists \alpha \in \{0,1\}^m : \, P = \left(\prod_i c_i^{\alpha_i}\right) P_0\}}{\arg\min} E(P)$$

$$C = \{c_1, \ldots, c_m\}$$

$$\boxed{E(Q,R) = \mathrm{vec}(Q)^T W \mathrm{vec}(R) \qquad P(\alpha) = P_0 + \sum_{i=1}^{m} \alpha_i \underbrace{(c_i - I) P_0}_{C_i}}$$

max planck institut informatik

Seelbach Benkner et al., ICCV 2021.

Shape Matching with AQC

Initialise P_0 via descriptor-based similarity

repeat until converged

obtain I_M and I_N and choose from them a set of *k* random and disjoint 2-cycles

construct a submatrix of worst matches W_s

repeat until every 2-cycle occurred

choose a random set of 2-cycles

calculate $\tilde{W}$ and solve $\min_{\alpha \in \{0,1\}^m} \alpha^\top \tilde{W} \alpha$ on QPU

$P_i = \left(\prod_j c_j^{\alpha_j} \right) P_{i-1}$

apply the obtained permutation to worst matches

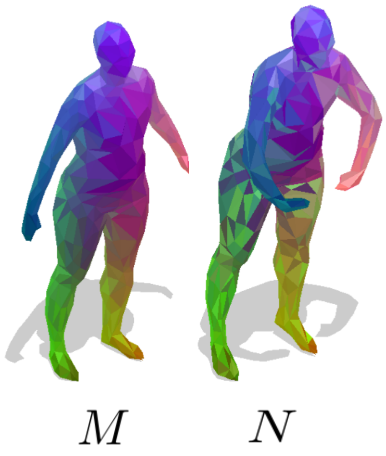

Seelbach Benkner et al., ICCV 2021.

Shape Matching with AQC

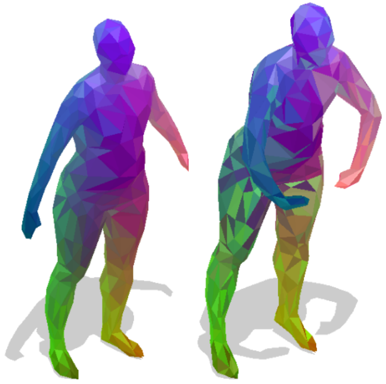

M N

Initialise P_0 via descriptor-based similarity

repeat until converged

obtain I_M and I_N and choose from them a set of *k* random and disjoint 2-cycles

construct a submatrix of worst matches W_s

repeat until every 2-cycle occurred

choose a random set of 2-cycles

calculate $\tilde{W}$ and solve $\min_{\alpha \in \{0,1\}^m} \alpha^\top \tilde{W} \alpha$ on QPU

$$P_i = \left(\prod_j c_j^{\alpha_j}\right) P_{i-1}$$

apply the obtained permutation to worst matches

NP-hard; decides to apply c_i or not

$$\begin{pmatrix} 1-\alpha_1 & 0 & \alpha_1 & 0 & 0 \\ \alpha_1 & 1-\alpha_1 & 0 & 0 & 0 \\ 0 & \alpha_1 & 1-\alpha_1 & 0 & 0 \\ 0 & 0 & 0 & 1-\alpha_2 & \alpha_2 \\ 0 & 0 & 0 & \alpha_2 & 1-\alpha_2 \end{pmatrix}$$

Seelbach Benkner et al., ICCV 2021.

Shape Matching with AQC

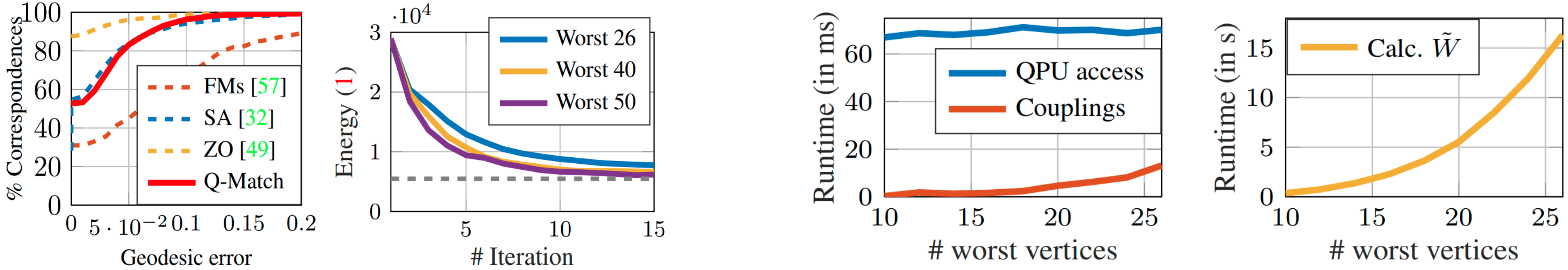

Accuracy and convergence (FAUST)

Runtime

Seelbach Benkner et al., ICCV 2021.

Shape Matching with AQC

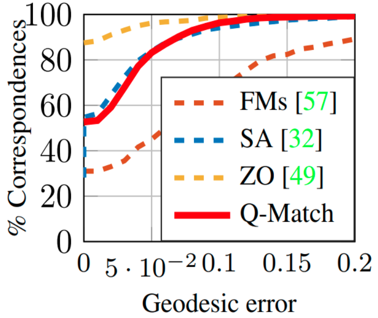

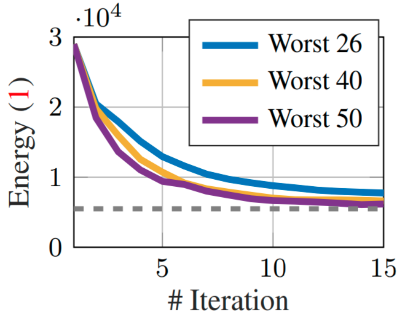

Accuracy and convergence (FAUST)

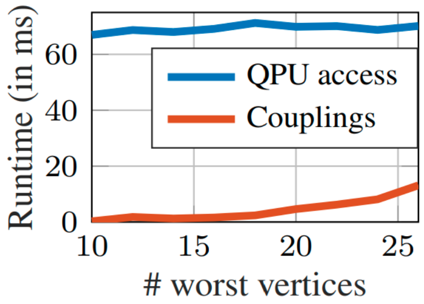

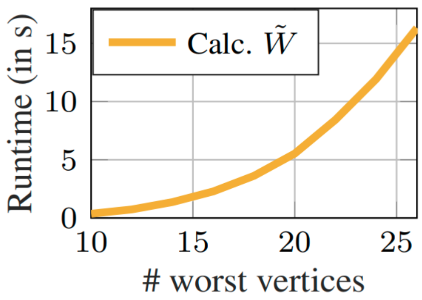

Runtime

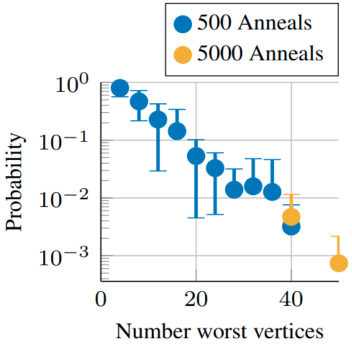

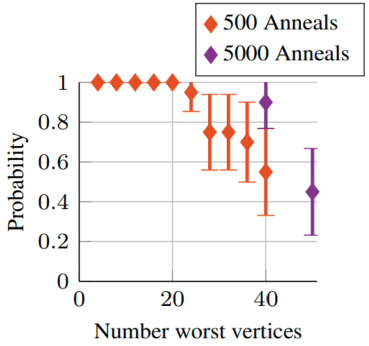

optimal solution probabilities

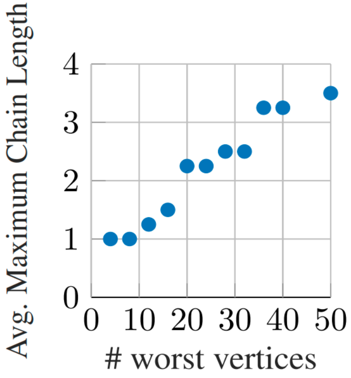

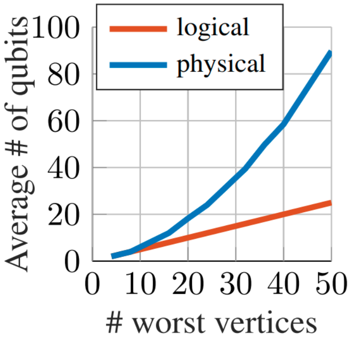

minor embedding statistics

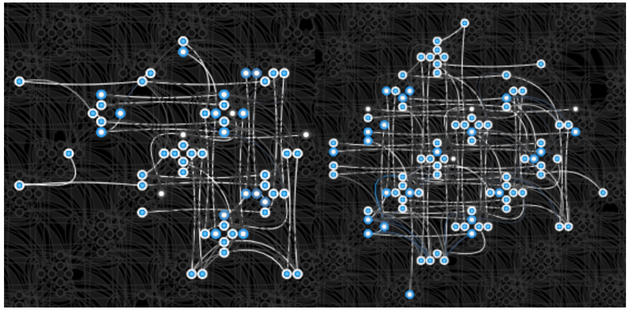

Minor embeddings
(40 and 50 vertices)

Seelbach Benkner et al., ICCV 2021.

WIP: Matching Multiple Shapes with AQC

cycle consistency

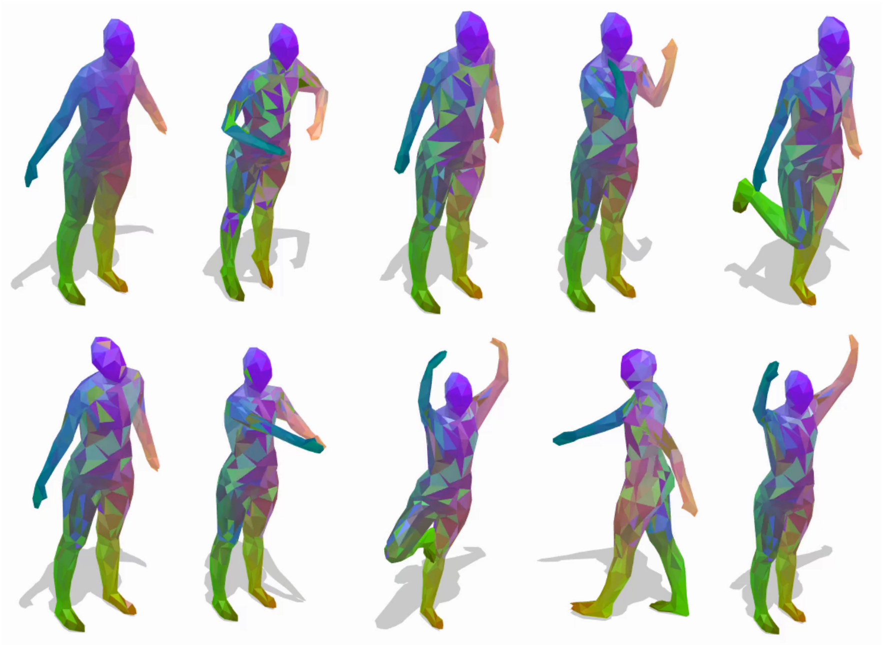

evolution of the matches

WIP: Quantum Annealing with Learnt Couplings

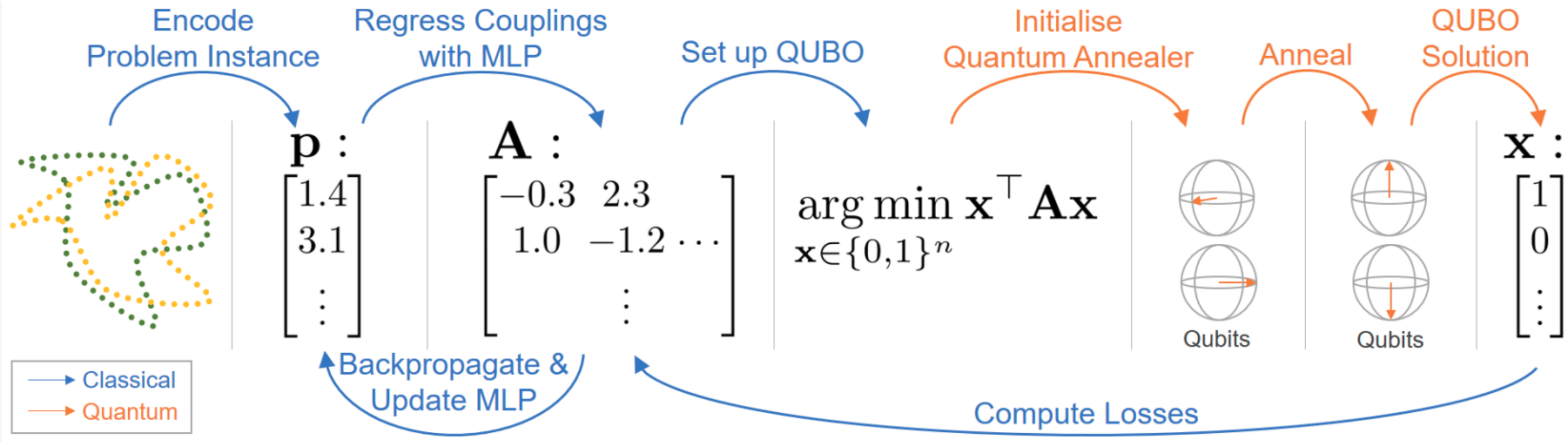

Seelbach Benkner et al., arXiv, 2022.

WIP: Quantum Annealing with Learnt Couplings

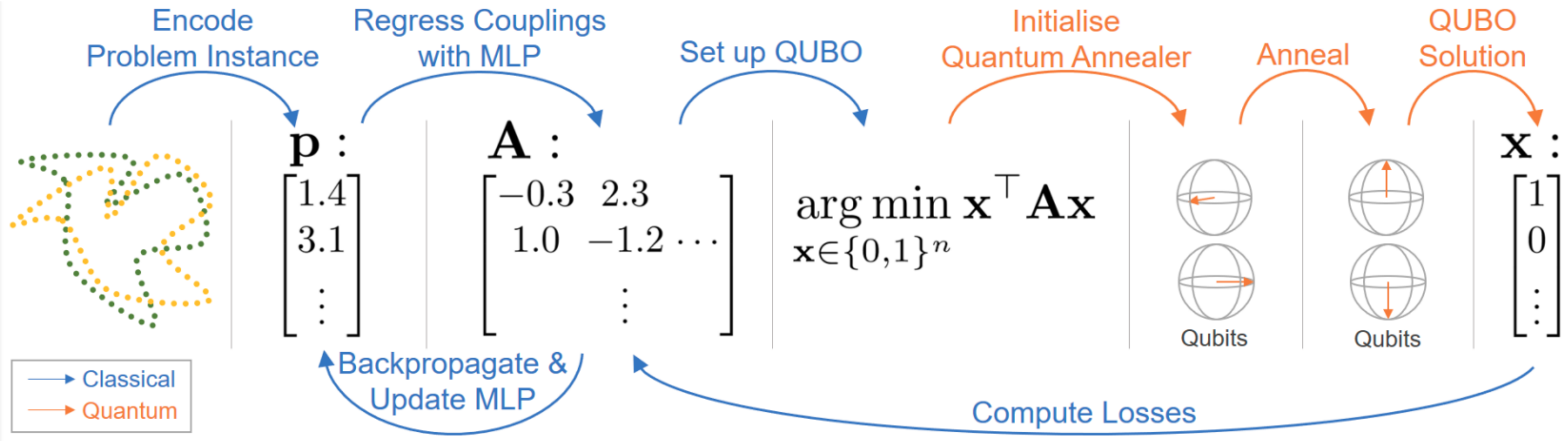

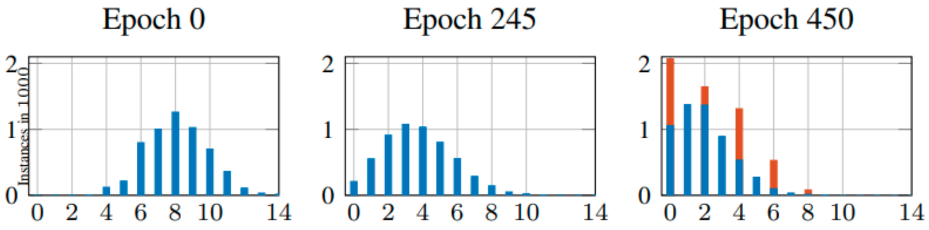

Hamming distance evolution over training epochs

Seelbach Benkner et al., arXiv, 2022.

Conclusion

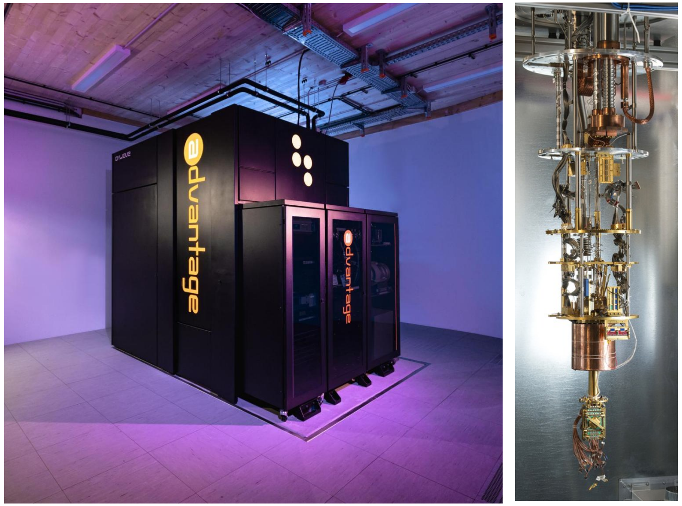

Copyright: Forschungszentrum Jülich

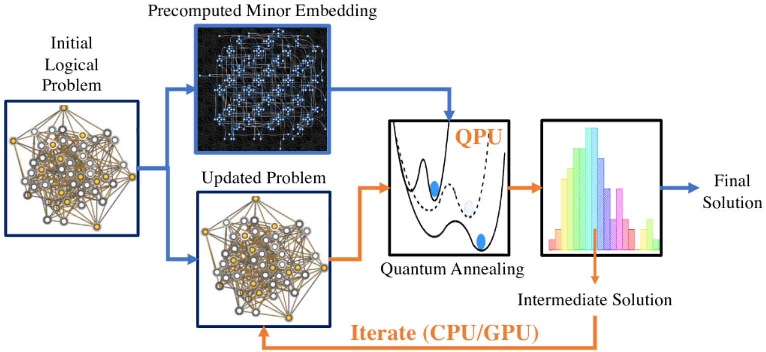

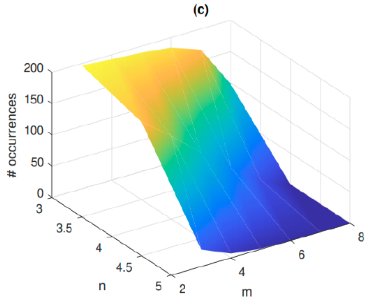

- QCV gains momentum
- QPUs as accelerators for CV, CG and ML
- Our mission: To enhance the visibility of QCV in the communities

References

[1] Shimada et al. **Neural Monocular 3D Human Motion Capture with Physical Awareness.** *ACM SIGGRAPH*, 2021.
[2] Shimada et al. **HULC: 3D Human Motion Capture with Pose Manifold Sampling and Dense Contact Guidance.** *ECCV*, 2022.
[3] Dabral et al. **Gravity-Aware Monocular 3D Human-Object Reconstruction.** *ICCV*, 2021.
[4] Li et al. **MoCapDeform: Monocular 3D Human Motion Capture in Deformable Scenes.** *3DV*, 2022.
[5] Tretschk et al. **Non-Rigid Neural Radiance Fields: Reconstruction and Novel View Synthesis of a Dynamic Scene From Monocular Video.** *ICCV*, 2021.
[6] Menapace et al. **Playable Environments: Video Manipulation in Space and Time.** *CVPR*, 2022.
[7] Tretschk and Kairanda et al. **State of the Art in Dense Monocular Non-Rigid 3D Reconstruction.** *ArXiv*, 2022.

[1] Seelbach Benkner et al. **Q-Match: Iterative Shape Matching via Quantum Annealing.** *ICCV*, 2021.
[2] Seelbach Benkner et al. **QuAnt: Quantum Annealing with Learnt Couplings.** *ArXiv*, 2022.
[3] Birdal and Golyanik et al. **Quantum Permutation Synchronization.** *CVPR*, 2021.
[4] Bhatia et al. **Generation of Truly Random Numbers on a Quantum Annealer.** *IEEE Access*, 2022.
[5] Arrigoni et al. **Quantum Motion Segmentation.** *ECCV*, 2022.

Thank You!